Electronic Supplementary Materials for

Breaking the Stability Barrier of Large Acenes

Monther Zreid,[a] Kaijie Ni,[b*] Jian-bin Lin,[a] Yuming Zhao,[a*]

[a]Department of Chemistry, Memorial University of Newfoundland

St. John's, NL, Canada A1B 3X7

Tel: +1 709 864 8747; Fax: 1 709 864 3702; Email: yuming@mun.ca

[b]College of Chemistry and Materials Engineering, Zhejiang Agriculture & Forestry University

Hangzhou, 311300, Zhejiang, China

Email: nikaijie@zafu.edu.cn

Contents

1 Experimental Section

1.1 General Information

All chemicals were purchased from commercial suppliers and used without further purification. Reactions were carried out in standard dry glassware under air or inert conditions. Solvent evaporation and concentration were performed using a rotary evaporator. Flash column chromatography was conducted using silica gel (240–400 mesh), and thin-layer chromatography (TLC) was performed on silica gel F254-coated plastic sheets, with visualization under UV light. Melting points (m.p.) were determined using an SRS OptiMelt melting point apparatus and are reported as uncorrected values.

1.2 Spectroscopic Characterization

^{1}H and ^{13}C NMR spectra were recorded on a Bruker Avance III 300 MHz or Burker NEO 500 MHz multinuclear spectrometer. Chemical shifts (δ) are reported in parts per million (ppm) relative to the internal standard tetramethylsilane ($SiMe_4$) or residual solvent signals ($CHCl_3$: $\delta_H = 7.26$ ppm, $\delta_C = 77.2$ ppm; CH_2Cl_2: $\delta_H = 5.32$ ppm, $\delta_C = 54.0$ ppm). Coupling constants (J) are reported in Hertz (Hz). Fourier-Transform infrared (FT-IR) spectra were acquired using a Bruker INVENIO-R spectrometer. High-resolution mass spectrometry (HRMS) was performed using an ESI-TOF (Agilent 1260 Infinity LC-6230) or an MALDI-TOF TOF (Bruker ultrafleXtreme) mass spectrometer.

1.3 Optical Characterization

UV-Vis-NIR absorption spectra were measured using a Cary 6000i spectrophotometer. Fluorescence spectroscopic analysis was performed on a Photon Technology International (PTI) QuantaMaster spectrophotometer.

The relative fluorescence quantum yields (Φ_F) of the samples were determined using quinine sulfate in 0.1 M H_2SO_4 ($\Phi = 0.54$) as the standard. Solutions of the sample and standard were prepared at absorbance below 0.10 at the excitation wavelength to minimize inner filter effects. The quantum yield of the sample (Φ_x) was calculated using the equation:

$$\Phi_F = \Phi_{\text{std}} \left(\frac{I_x}{I_{\text{std}}} \right) \left(\frac{A_{\text{std}}}{A_x} \right) \left(\frac{n_x^2}{n_{\text{std}}^2} \right),$$

where I, A, and n represent the integrated fluorescence intensity, absorbance at the excitation wavelength, and refractive index of the solvent, respectively.

1.4 Electrochemical Analysis

Electrochemical measurements, including cyclic voltammetry (CV) and differential pulse voltammetry (DPV), were performed using a BASi Epsilon electrochemical analyzer. A three-electrode system was employed, consisting of a glassy carbon working electrode, a platinum (Pt) wire counter electrode, and an Ag/AgCl reference electrode. The electrolyte solution was prepared using BuN_4BF_4 (0.10 M) as the supporting electrolyte. All experiments were conducted at room

temperature, and the solutions were purged with nitrogen gas for ca. 5 min prior to measurements to remove dissolved oxygen.

1.5 X-ray Crystallographic Analysis

Single-crystal X-ray diffraction (SCXRD) data were collected at 293(2) K on an XtaLAB Synergy-S, Dualflex, HyPix-6000HE diffractometer using Cu Kα radiation ($\lambda = 1.5406$ Å). The crystal sample was mounted on nylon CryoLoops with Paraton-N. Data collection and reduction were processed using *CrysAlisPro* (Rigaku OD, 2021). A multi-scan absorption correction was applied to the collected reflections. The structure was solved using the *SHELXT*[1] software package via intrinsic phasing and refined with the *SHELXL*[2] refinement package using least-squares minimization, both implemented within the *OLEX2* software package.[3] All non-hydrogen atoms were refined anisotropically, while hydrogen atoms attached to organic moieties were generated geometrically.

1.6 Electron Paramagnetic Resonance Analysis

Electron Paramagnetic Resonance (EPR) spectroscopy was performed using a Bruker EMXplus-6/1 X-band EPR spectrometer equipped with a high-sensitivity resonator. The EPR spectra were acquired and analyzed using Bruker's Xenon software.

The following experimental conditions were employed: microwave frequency = 9.825759 GHz, microwave power = 6.325 mW, modulation frequency = 100 kHz, modulation amplitude = 3.000 Gauss, center field = 3505.00 Gauss, sweep width = 100.0 Gauss, number of scans = 3, receiver gain = 30 dB, time constant = 0.01 ms, sweep time = 30.00 s, field range = 3455.000–3554.900 Gauss, resolution = 1000 points.

1.7 Magnetic Properties Measurements

The magnetic properties of the samples were investigated using a Superconducting Quantum Interference Device (SQUID) magnetometer. The measurements were performed on a Physical Property Measurement System (PPMS-9) from Quantum Design, USA. The following experimental conditions and parameters were employed:

- Sample cavity size: Net inner diameter not less than 25 mm.
- Magnetic field Strength: Longitudinal magnet with a range of $\pm$ 9 Tesla.
- Scanning speed: Adjustable from 1 to 200 Gauss s^{-1}.
- Magnetic field resolution: 0.02 mTesla.
- Temperature control range: 1.9–400 K.
- Temperature scanning speed: Adjustable from 0.01 to 12 K min^{-1}.
- Temperature stability:

- ⋆ $\pm 0.2\%$ when the temperature is below 10 K.
- ⋆ $\pm 0.02\%$ when the temperature is above 10 K.

1.8 Computational Methods

Single-point density functional theory (DFT) calculations were performed on compound **12** using the geometric parameters obtained from X-ray crystallographic analysis. To reduce computational cost, the triisopropylsilyl (TIPS) groups were replaced with hydrogen atoms. The calculations were carried out using the B3LYP functional combined with the 6-311+G(2d,p) basis set, as implemented in the *Gaussian 16* software package[4].

Nuclear magnetic resonance (NMR) shielding properties were computed using the Gauge-Independent Atomic Orbital (GIAO) method[5,6]. The formatted checkpoint (.fchk) files generated from the *Gaussian 16* calculations were further processed using the *Multiwfn* software package[7] to visualize the $NICS_{ZZ}(1)$ map, which provides insights into the aromaticity of the system. Additionally, the Anisotropy of the Induced Current Density (AICD) plot for compound **12** was generated using the AICD program (version 3.0.4) developed by the Herges group (`https://www.otto-diels-institut.de/herges/pages_en/projects_acid.html`). This analysis aids in visualizing the induced current density and assessing the magnetic response of the molecule.

The Harmonic Oscillator Model of Aromaticity (HOMA) is calculated using the formula:

$$\text{HOMA} = 1 - \frac{1}{N}\sum_{i=1}^{N}\left(\frac{R_{\text{opt}} - R_i}{\alpha}\right)^2$$

where R_{opt} represents the optimal bond length for full aromaticity (1.388 Å), R_i denotes the observed bond lengths, N is the number of bonds, and α is an empirical scaling factor (257.7 Å^{-2}).[8? –10]

2 Synthetic Procedures

Compound S1

To a round-bottomed flask (1.0 L) were added 1,4,5,8-tetramethoxyanthracene (8.0 g, 27 mmol) and THF (300 mL). The resulting suspension was stirred with a magnetic bar at rt. A solution of $NaIO_4$ (7.5 g, 34.9 mmol, 1.3 equiv) in deionized water (100 mL) was added, and then H_2SO_4 (conc., 2 mL) was added dropwise. After addition, the reaction mixture was heated to 80 °C and maintained at this temperature for 4 h. Subsequently, the system was allowed to cool down to room temperature and stirred for an additional 1 h. The reaction mixture was then subjected to suction filtration, and the obtained solid product was dried in air, affording compound **S1** as a red crystalline solid (6.0 g, 22.4 mmol, 83%). m.p. 212.8 °C (decomp.). FTIR (neat): 2952, 2845, 1663, 1613, 1471, 1437, 1385, 1333, 1299, 1270, 1244, 1233, 1214, 1173, 1146, 1116, 1086, 1057, 1020, 963, 927, 847, 821, 721, 704, 595, 565, 463, 446, 411 cm^{-1}. ^{1}H NMR (300 MHz, $CDCl_3$): δ 8.97 (s, 2H), 7.05 (s, 2H), 6.89 (s, 2H), 3.99 (s, 6H). ^{13}C NMR (75 MHz, $CDCl_3$): δ

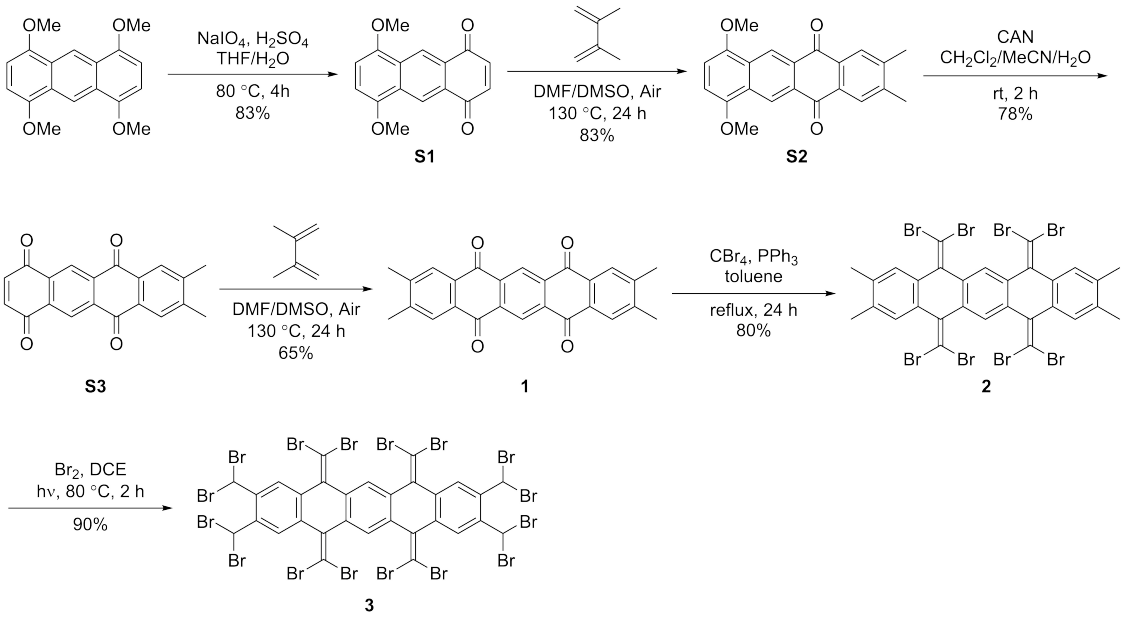

Figure S-1: Synthetic route to precursor **3**.

184.93, 151.08, 140.14, 128.21, 127.73, 123.58, 107.64, 56.05. HRMS (ESI-TOF, positive mode): m/z calcd for $C_{16}H_{13}O_4$ [M + H]$^+$: 269.0808; found: 269.0807.

Compound S2

Compound **S1** (6.77 g, 25.3 mmol) was suspended in a mixture of DMSO and DMF (400 mL, 1:1 v/v) and stirred at rt. To this suspension, boron trifluoride etherate ($BF_3{\cdot}OEt_2$, 2 mL, 1:3 v/w) was added, followed by 2,3-dimethyl-1,4-butadiene (5.7 mL, 50.5 mmol, 2 equiv). The reaction mixture was heated to 130 °C under a continuous flow of air and maintained at this temperature for 24 h. The reaction was then cooled down to rt, and to the cooled solution was slowly added methanol (400 mL). The reaction mixture was further stirred for 1 h, followed by suction filtration. The obtained solids were washed with methanol (5 × 100 mL), and dried in air, yielding compound **S2** (7.3 g, 21 mmol, 83.4%) as an orange-color crystalline solid. m.p. 204.0 °C (decomp.). FTIR (neat): 2939, 2834, 1669, 1601, 1584, 1469, 1434, 1386, 1336, 1321, 1295, 1268, 1221, 1197, 1169, 1146, 1111, 1090, 1036, 984, 956, 929, 899, 809, 738, 715, 599, 511, 439, 420 cm^{-1}. ^{1}H NMR (300 MHz, $CDCl_3$): δ 9.16 (s, 2H), 8.12 (s, 2H), 6.86 (s, 2H), 4.00 (s, 6H), 2.44 (s, 6H). ^{13}C NMR (75 MHz, $CDCl_3$): δ 183.16, 150.85, 143.92, 132.58, 129.72, 128.36, 127.93, 123.76, 107.03, 55.89, 20.22. HRMS (ESI-TOF, positive mode): m/z calcd for $C_{22}H_{19}O_4$ [M + H]$^+$: 347.1278; found: 347.1273.

Compound S3

In a round-bottomed flask, compound **S2** (5.50 g, 15.9 mmol) was suspended in a mixture of CH_2Cl_2 (400 mL) and CH_3CN (50 mL). To this mixture was added a solution of $(NH_4)_2[Ce(NO_3)_6]$ (26.0 g, 47.7 mmol, 3 equiv) in water (25 mL) in a dropwise manner. The reaction mixture was stirred at rt for 1 hour (the reaction mixture was observed to gradually change from orange to

dark brown in color). The reaction mixture was kept under stirring for another 1 h, resulting in a bright yellow solution and the formation of yellow crystalline precipitates. The completion of the reaction was confirmed with TLC (CH_2Cl_2/hexanes, 4:1) analysis. The yellow crystalline solid was collected by suction filtration, washed sequentially with CH_2Cl_2 (100 mL) and methanol (3 $\times$ 100 mL), and then air-dried to afford compound **S3** (3.25 g). The filtrate was washed with water, and the organic layer was dried over anhydrous $MgSO_4$, concentrated under reduced pressure, and purified by flash column chromatography (CH_2Cl_2/hexanes, 4:1) to yield an additional amount of **S3** (0.66 g). Totally, compound **S3** (3.91 g, 12.4 mmol, 78%) was obtained as a yellow crystalline solid. m.p. 185.8 °C (decomp.). FTIR (neat): 3058, 1664, 1605, 1466, 1398, 1385, 1360, 1349, 1337, 1321, 1290, 1218, 1123, 1083, 1045, 1025, 969, 944, 902, 845, 736, 707, 686, 603, 561, 491, 427 cm^{-1}. ^1H NMR (300 MHz, $CDCl_3$): δ 8.95 (s, 2H), 8.07 (s, 2H), 7.13 (s, 2H), 2.46 (s, 6H). ^{13}C NMR (75 MHz, $CDCl_3$): δ 183.60, 181.76, 145.27, 139.41, 136.99, 135.01, 131.48, 128.75, 126.42, 20.49. HRMS (ESI-TOF, positive mode): m/z calcd for $C_{20}H_{13}O_4$ $[M + H]^+$ 317.0808, found 317.0806.

Compound 1

Compound **S3** (3.20 g, 10.1 mmol) was suspended in a mixture of DMSO/DMF (200 mL, 1:1 v/v) and stirred at rt. To this suspension were sequentially added $BF_3{\cdot}OEt_2$ (1 mL, 1:3 v/w) and 2,3-dimethyl-1,4-butadiene (2.3 mL, 20.2 mmol, 2 equiv). The reaction mixture was heated at 130 °C for 24 h under continuous airflow. After this, methanol (200 mL) was added slowly to the reaction mixture, and the resulting suspension was allowed to cool to rt over a period of 1 with continuous stirring. Dark red solids precipitated out of the solution, which was collected by suction filtration, washed with methanol (5 $\times$ 100 mL), and air-dried to yield compound **1** (2.60 g, 6.6 mmol, 65%) as a dark red solid. m.p. 211.0 °C (decomp.). FTIR (neat): 3058, 2949, 2919, 1675, 1593, 1447, 1374, 1338, 1321, 1288, 1201, 1130, 1082, 1027, 1009, 981, 947, 925, 902, 745, 719, 695, 585, 565, 492, 445, 417 cm^{-1}. ^1H NMR (300 MHz, $CDCl_3$): δ 9.19 (s, 2H), 8.13 (s, 4H), 2.48 (s, 12H). HRMS (ESI-TOF, positive mode): m/z calcd for $C_{26}H_{19}O_4$ $[M + H]^+$ 395.1278, found 395.1264.

Compound 2

A solution of CBr_4 (13.5 g, 40.6 mmol, 16 equiv) in toluene (200 mL) was prepared and kept stirring at rt in a 500 mL round-bottomed flask. To this solution, PPh_3 (21.3 g, 81.2 mmol, 32 equiv) was added. The reaction mixture was stirred at rt for another 30 min. Subsequently, compound **1** (1.0 g, 2.5 mmol) was added to the reaction mixture in one portion, and the reaction was heated to reflux under stirring for 48 h. After this, the reaction was allowed to cool down to rt and filtered via suction filtration. The filtrate was evaporated under reduced pressure, and the resulting solid was suspended in methanol (100 mL) and allowed to settle for 30 min. The suspension was subjected to suction filtration and the collected solid was air-dried, affording compound **2** (2.10 g, 2.06 mmol, 80%) as a beige solid. m.p. 200.0 °C (decomp.). ^1H NMR (500 MHz, $CDCl_3$): δ 7.77 (s, 4H), 6.15 (s, 2H), 2.53 (s, 12H). ^{13}C NMR (126 MHz, $CDCl_3$): δ 138.92, 136.44, 134.05, 132.89, 128.48, 125.25, 90.37, 20.96. FTIR (neat): 2916, 1565, 1473, 1449, 1383, 1012, 954, 906, 882, 784, 754, 639, 617, 594, 478, 429 cm^{-1}.

Compound 3

To an oven-dried 500 mL round-bottomed flask was charged compound **2** (3.8 g, 3.7 mmol) and 1,2-dichloroethane (100 mL). The suspension was stirred and heated to 80 °C under direct irradiation with a halogen lamp (50 W, Dollarama). Bromine (14.3 g, 4.60 mL, 89.7 mmol, 24 equiv) was added dropwise into the reaction mixture, resulting in a dark red solution, which was stirred at 80 °C under continuous irradiation for 3 h. The completion of the reaction was confirmed by TLC analysis (CH_2Cl_2/hexanes, 3:7). The reaction mixture was allowed to cool down to rt, and methanol (100 mL) was carefully added to induce further precipitation. Finally, the precipitates were collected via suction filtration, washed with methanol (3 × 100 mL), and air-dried, affording compound **3** (5.55 g, 3.40 mmol, 90%) as a white solid. m.p. 211.0 °C (decomp.). FTIR (neat): 3021, 1575, 1472, 1457, 1396, 1318, 1211, 1182, 1132, 1005, 970, 909, 822, 781, 750, 711, 669, 657, 631, 497, 458 cm^{-1}. Due to the very low solubility of the product in organic solvents, NMR characterization could not be achieved.

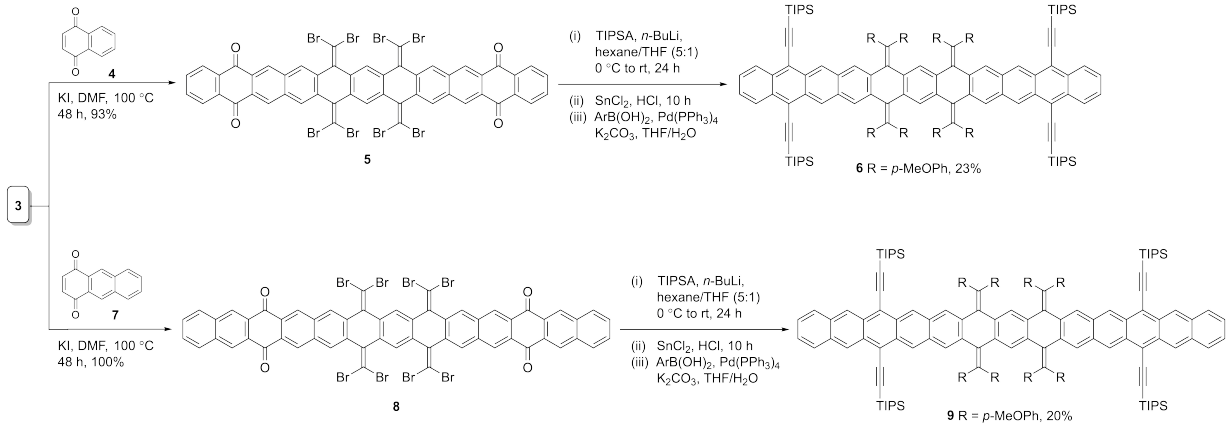

Figure S-2: Synthetic route to undecacenes **6** and tridecacenes **9**.

Compound 5

To a flame-dried 50 mL round-bottomed flask was charged compound **3** (0.5 g, 0.3 mmol), 1,4-naphthoquinone (**4**, 0.1 g, 0.6 mmol, 2.1 equiv), KI (0.71 g, 4.2 mmol, 14 equiv), and DMF (10 mL). The mixture was flushed with dry nitrogen gas for 20 min and then sealed with a septum. Under a nitrogen atmosphere, the reaction mixture was heated at 100 °C for 48 h. Completion of the reaction was confirmed with TLC (CH_2Cl_2/hexane, 4:1) analysis. Methanol (10 mL) was then added to the reaction mixture, and the resulting mixture was stirred at rt for another 1 h and subjected to suction filtration. The collected solids were washed sequentially with water (3 × 20 mL) and methanol (3 × 20 mL), and dried under vacuum, affording compound **5** (0.37 g, 0.28 mmol, 93%) as a yellow solid. m.p. 185.0 °C (decomp.). FTIR (neat): 3066, 1675, 1619, 1587, 1436, 1397, 1319, 1274, 1160, 999, 971, 933, 902, 807, 781, 710, 638, 615, 481 cm^{-1}. ^{1}H NMR (300 MHz, $CDCl_3$): δ 8.98 (s, 4H), 8.63 (s, 4H), 8.39 (m, 4H), 7.83 (m, 4H), 7.14 (s, 2H). ^{13}C NMR (75 MHz, $CDCl_3$): δ 182.52, 137.79, 135.94, 134.46, 134.41, 134.36, 133.25, 130.95, 129.87, 128.96, 127.66, 126.55, 93.43.

Compound 8

To a flame-dried 50 mL round-bottomed flask was charged compound **3** (0.5 g, 0.3 mmol), 1,4-anthraquinone (**7** (0.13 g, 0.6 mmol, 2.1 equiv), KI (0.71 g, 4.2 mmol, 14 equiv), and DMF (10 mL). The mixture was flushed with dry nitrogen gas for 20 min and then sealed with a septum. Under a nitrogen atmosphere, the reaction was heated at 100 °C for 48 h. Completion of the reaction was confirmed by TLC (CH_2Cl_2). Methanol (10 mL) was added to the reaction mixture, which was then stirred at rt for another 1 hour. The resulting precipitates were collected by suction filtration, washed sequentially with water (3 × 20 mL) and methanol (3 × 20 mL), and dried under vacuum, affording compound **8** (0.43 g, 0.30 mmol, 100%) as a brownish solid. An analytically pure sample was obtained by passing 20 mg of the product through a short plug of silica gel using CH_2Cl_2 as the eluent. m.p. 183.0 °C (decomp.). FTIR (neat): 3052, 2920, 2450, 1677, 1615, 1582, 1452, 1435, 1392, 1265, 1214, 1183, 991, 959, 933, 812, 780, 856, 638, 609, 569, 551, 475 cm^{-1}. ^1H NMR (300 MHz, $CDCl_3$): δ 9.03 (s, 4H), 8.89 (s, 4H), 8.64 (s, 4H), 8.07 (m, 4H), 7.68 (m, 4H), 7.22 (s, 2H). ^{13}C NMR (75 MHz, $CDCl_3$): δ 182.47, 137.88, 135.96, 135.29, 134.55, 133.32, 131.76, 130.35, 130.16, 130.02, 129.67, 128.97, 126.66, 93.40.

Compound 6

To a flame-dried 250 mL round-bottomed flask, under a nitrogen atmosphere, was charged TIPS-acetylene (1 mL, 4.5 mmol, 16 equiv) and dry hexane (100 mL). The mixture was cooled to 0 °C with an ice-water bath, and *n*-BuLi (1.7 mL, 4.2 mmol, 15 equiv) was added dropwise. The reaction mixture was stirred at 0 °C for 30 min and then at rt for additional 1.5 h. To the reaction mixture was added compound **5** (0.37 g, 0.28 mmol) in one portion, followed by addition of dry THF (20 mL). The reaction flask was wrapped with aluminum foil to avoid exposure to light. The reaction mixture was further stirred at rt 24 h. After this, the reaction was quenched by adding 1 mL of degassed saturated NH_4Cl solution. A solution of anhydrous $SnCl_2$ (0.85 g, 4.5 mmol, 16 equiv) in HCl (3.0 M, 10 mL) was flushed with nitrogen gas for 3 min and then added to the reaction mixture. The resulting mixture was stirred in the dark under nitrogen for 10 h. During this period, the reaction solution was observed to turn into a deep red suspension. CH_2Cl_2 (150 mL) was added, and the mixture was washed with water. The organic layer was collected and dried over anhydrous $MgSO_4$, filtered, and concentrated under vacuum. The resulting red solid was suspended in methanol (100 mL), filtered, and collected by suction filtration. The obtained red solid was used directly in the subsequent Suzuki cross-coupling reaction without further purification.

In a 250 mL round-bottomed flask, the red solid (0.45 g), $Pd(PPh_3)_4$ (0.026 g, 0.023 mmol, 0.1 equiv), a K_2CO_3 solution (2.0 M, 25 mL), and THF (75 mL) were combined and flushed with nitrogen gas for 20 min. To the reaction mixture was added 4-methoxyphenyl boronic acid (0.55 g, 3.6 mmol, 16 equiv) in one portion, and the reaction flask was sealed and heated at 90 °C for 48 h. After completion, the reaction mixture was washed with water (50 mL), and the organic layer was collected, dried over anhydrous $MgSO_4$, and concentrated under vacuum. The crude product was purified by flash column chromatography (EtOAc/hexanes, 1.5:8.5 v/v) to yield compound **6** (0.10 g, 0.060 mmol, 23%) as a red solid. m.p. 159.0 °C (decomp.). FTIR (neat): 2941, 2890, 2862, 2834, 2145, 2120, 1604, 1571, 1507, 1461, 1381, 1284, 1243, 1173, 1105, 1074, 1037, 993, 906, 882, 843, 816, 764, 745, 669, 655, 627, 601, 588, 508, 562 cm^{-1}. ^1H NMR (300 MHz, CD_2Cl_2): δ 8.87 (s, 4H), 8.64–8.55 (m, 4H), 7.61 (s, 4H), 7.57–7.49 (m, 4H), 7.31–7.23 (m, 8H),

7.19–7.10 (m, 8H), 6.86–6.77 (m, 16H), 6.75 (s, 2H), 3.69, 3.70 (2s, 24H), 1.43–1.32 (m, 84H). ^{13}C NMR (75 MHz, CD_2Cl_2): δ 159.08, 158.77, 140.37, 137.33, 135.63, 135.58, 135.52, 134.96, 132.83, 131.07, 131.00, 130.89, 130.55, 128.18, 127.69, 127.16, 127.07, 126.03, 118.65, 114.16, 113.89, 106.30, 104.21, 55.73, 55.44, 19.25, 12.08. HRMS (MALDI+, DCTB): m/z calcd. for $C_{150}H_{158}Si_4O_8$ $[M]^+$: 2199.10283, found: 2199.10334; correct isotope distribution.

Compound 9

To a flame-dried 250 mL round-bottom flask, under a nitrogen atmosphere, were charged TIPS – acetylene (1.1 mL, 4.8 mmol, 16 equiv), and dry hexane (100 mL). The mixture was cooled down to 0 °C, and *n*-BuLi (1.8 mL, 4.5 mmol, 15 equiv) was added dropwise. The reaction mixture was stirred at 0 °C for 30 min and then at rt for an additional 1.5 h. Compound **8** (0.43 g, 0.30 mmol) was added in one portion, followed by addition of dry THF (20 mL). The reaction flask was wrapped with aluminum foil to avoid exposure to light, and the reaction mixture was stirred for 24 h and then quenched by adding 1 mL of degassed saturated NH_4Cl solution. A solution of anhydrous $SnCl_2$ (0.92 g, 4.8 mmol, 16 equiv) in HCl (3.0 M, 10 mL) was flushed with nitrogen gas for 3 min and then added to the reaction mixture. The reaction mixture was stirred in the dark under a nitrogen atmosphere for 10 h. During this period, the reaction solution was observed to change into a dark green suspension. CH_2Cl_2 (150 mL) was added, and the mixture was washed with water. The organic layer was collected, dried over $MgSO_4$, filtered, and concentrated under reduced pressure. The resulting green solid was suspended in methanol (100 mL), filtered, and collected by suction filtration. The obtained solid was used directly in the subsequent Suzuki cross-coupling reaction without further purification.

In a 250 mL round-bottomed flask, the green solid (0.53 g), $Pd(PPh_3)_4$ (29 mg, 0.025 mmol, 0.1 equiv), K_2CO_3 solution (2.0 M, 25 mL), and THF (75 mL) were combined and flushed with nitrogen gas for 20 min. To the reaction mixture was added 4-methoxyphenylboronic acid (0.62 g, 4.1 mmol, 16 equiv) in one portion, and the reaction flask was sealed and heated at 90 °C for 48 h. After completion, the reaction mixture was washed with water (50 mL), and the organic layer was collected, dried over $MgSO_4$, and concentrated under vacuum. The crude product was purified by flash column chromatography (EtOAc/hexane, 1.5:8.5 v/v) to afford compound **9** (0.10 g, 0.060 mmol, 20%) as a green solid. m.p. 222.0 °C (decomp.). FTIR (neat): 2939, 2862, 2834, 2134, 1604, 1572, 1506, 1461, 1368, 1284, 1244, 1174, 1137, 1105, 1072, 1037, 1012, 996, 909, 879, 844, 822, 769, 740, 675, 589, 574, 508, 463 cm^{-1}. ^{1}H NMR (300 MHz, CD_2Cl_2): δ 9.26 (s, 4H), 8.85 (s, 4H), 7.99–7.96 (dd, $J = 6.6, 3.2$ Hz, 5H), 7.55 (s, 4H), 7.45–7.39 (m, 4H), 7.32–7.23 (m, 8H), 7.18–7.11 (m, 8H), 6.85–6.77 (m, 16H), 6.73 (s, 2H), 3.71 and 3.69 (2s, 24H), 1.42–1.39 (m, 84H). ^{13}C NMR (75 MHz, CD_2Cl_2): δ 159.08, 158.79, 140.42, 137.32, 135.60, 135.56, 135.52, 134.93, 132.65, 131.07, 130.99, 130.88, 130.82, 128.95, 128.25, 127.19, 126.56, 125.98, 118.36, 114.17, 113.89, 107.64, 104.95, 55.74, 55.45, 19.29, 12.16. HRMS (MALDI+, DCTB): m/z calcd. for $C_{158}H_{162}Si_4O_8$ $[M]^+$: 2299.13413; found: 2299.12624. Isotope distribution matched the calculated pattern.

Compound 10

Compound **1** (0.500 g, 1.27 mmol) was suspended in CH_2Cl_2 (100 mL), and the mixture was stirred at rt under the irradiation of a halogen lamp (50 W). Bromine (4.9 g, 1.6 mL, 30.4 mmol, 24

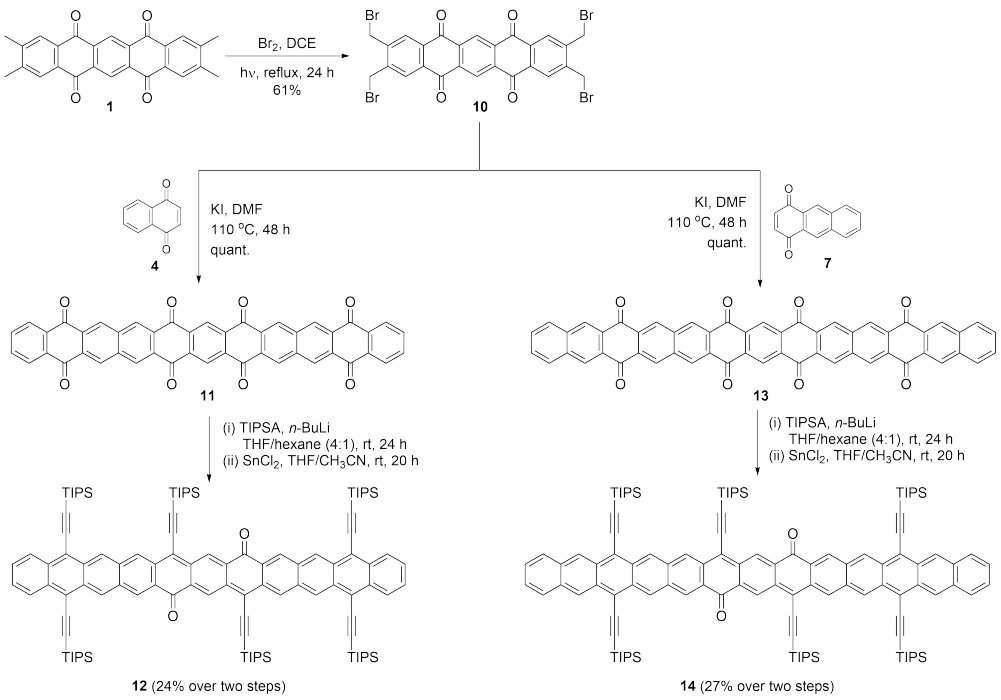

Figure S-3: Synthetic routes to undecacene **12** and tridecacene **14**.

equiv) was added dropwise, and the mixture was heated to reflux under stirring for 24 h. After this, the reaction mixture was subjected to suction filtration, and the filtrate was collected and passed through a short plug of silica gel, using CH_2Cl_2 as the eluent. The yellow colored fraction was collected and concentrated under vacuum, resulting in a yellow solid. This solid was suspended in methanol (100 mL) and then collected through suction filtration, affording compound **10** (0.55 g, 0.8 mmol, 61%) as a yellow crystalline solid. An analytically pure sample of **10** was obtained by recrystallization from a hot DMF solution. m.p. 209.0 °C (decomp.). FTIR (neat): 3038, 1674, 1598, 1467, 1325, 1281, 1216, 1197, 1137, 1001, 954, 817, 747, 721, 660, 625, 579, 553, 497, 444, 411 cm^{-1}. ^1H NMR (500 MHz, $CDCl_3$): δ 9.27–9.25 (m, 2H), 8.41 (s, 4H), 4.80 (s, 8H). HRMS (MALDI+,DHP/CHCA): *m/z* calcd. for $C_{26}H_{15}Br_4O_4$: $[M]^+$ 706.76983, found: 706.77085, correct isotope distribution.

Compound 11

To a flame-dried 50 mL round-bottomed flask were charged compound **10** (0.20 g, 0.28 mmol), 1,4-naphthoquinone (**4**, 0.093 g, 0.59 mmol, 2.1 equiv), KI (0.65 g, 3.9 mmol, 14 equiv), and DMF (5 mL). The mixture was flushed with dry nitrogen gas for 10 min and then the reaction flask sealed with a septum. The reaction mixture was kept under a nitrogen atmosphere and heated at 100 °C for 48 h. During this period, yellow-greenish precipitates gradually formed. The reaction was allowed to cool down to rt and stirred for another 30 min. The resulting yellow-greenish solid was collected by suction filtration, washed sequentially with water (3 × 20 mL), acetone (3 × 20 mL), and methanol (3 × 20 mL), and then dried under vacuum, affording compound **11** (0.19 g, 0.28 mmol, 100%) as a yellow solid. m.p. 253.0 °C (decomp.). FTIR (neat): 3065, 3036, 1672, 1583, 1467, 1393, 1329, 1267, 1194, 1160, 1001, 960, 792, 718, 480, 444 cm^{-1}.

Compound 12

To a flame-dried 100 mL round-bottomed flask, under a nitrogen atmosphere, were charged TIPSA (4.60 mL, 20.6 mmol, 96 equiv) and dry hexane (10 mL). The mixture was cooled down to 0 °C, and *n*-BuLi (2.5 M, 7.7 mL, 19.3 mmol, 90 equiv) was added dropwise. The reaction mixture was stirred at 0 °C for 30 min and then at rt for an additional 3 h. Compound **11** (0.15 g, 0.21 mmol) was added in one portion, followed by addition of dry THF (40 mL). The reaction flask was wrapped with aluminum foil to avoid exposure to light. The reaction mixture was stirred for 24 h and quenched with aq. HCl (1 M, 10 mL). The organic layer was collected, dried over anhydrous $MgSO_4$, and concentrated under reduced pressure. A dark orange crude product was obtained, which was redissolved in a mixture of dry THF/CH_3CN (10 mL, 1:1 v/v) under a nitrogen atmosphere. To this solution was added anhydrous $SnCl_2$ (0.65 g, 3.4 mmol, 16 equiv), and the reaction mixture was stirred at rt in the dark for 20 h. Dark blue solids were formed, which were collected by suction filtration, washed with a 1:1 mixture of THF/CH_3CN until the filtrate became colorless, and then dried under vacuum to afford pure compound **12** (0.08 g, 0.05 mmol, 24%) as a dark blue solid. m.p. 166.4 °C (decomp.). FTIR (neat): 3566, 2941, 2889, 2863, 2143, 2124, 1662, 1594, 1524, 1500, 1461, 1381, 1313, 1255, 1177, 1069, 1039, 1016, 995, 938, 919, 900, 881, 835, 797, 759, 731, 671, 592, 513, 459 cm^{-1}. HRMS (MALDI+, DCTB): m/z calcd. for $C_{112}H_{144}Si_6O_2$ $[M]^+$: 1688.97764, found: 1688.97807; correct isotope distribution.

Compound 13

To a flame-dried 50 mL round-bottomed flask were charged compound **10** (0.20 g, 0.28 mmol), 1,4-anthraquinone (**7**, 0.123 g, 0.59 mmol, 2.1 equiv), KI (0.65 g, 3.9 mmol, 14 equiv), and DMF (5 mL). The mixture was flushed with dry nitrogen gas for 10 min and then the flask was sealed with a septum. The reaction mixture was kept under a nitrogen atmosphere and heated at 100 °C for 48 h. During this period, greenish precipitated gradually formed. The reaction was allowed to cool down to rt and stirred for another 30 min. The resulting greenish solids were collected by suction filtration, washed sequentially with water (3 × 20 mL), acetone (3 × 20 mL), and methanol (3 × 20 mL), and dried under vacuum, affording compound **12** (0.22 g, 0.28 mmol, 100%) as a greenish solid. m.p. 235.0 °C (decomp.). FTIR (neat): 3055, 1674, 1617, 1578, 1455, 1392, 1330, 1268, 1184, 987, 959, 757, 718, 567, 476, 444 cm^{-1}.

Compound 14

To a flame-dried 100 mL round-bottomed flask, under a nitrogen atmosphere, were charged TIPSA (5.4 mL, 24 mmol, 96 equiv) and dry hexane (10 mL). The mixture was cooled down to 0 °C, and *n*-BuLi (2.5 M, 9.0 mL, 22.5 mmol, 90 equiv) was added dropwise. The reaction mixture was stirred at 0 °C for 30 min and then at rt for an additional 3 h. Compound **13** (0.20 g, 0.25 mmol) was added in one portion, followed by addition of dry THF (40 mL). The reaction flask was wrapped with aluminum foil to avoid exposure to light. The reaction mixture was stirred for 24 h and then quenched with aq. HCl (1.0 M, xx mL). The organic layer was collected, dried over anhydrous $MgSO_4$, and concentrated under reduced pressure. Dark orange crudes were obtained, which were redissolved in a mixture of dry THF/CH_3CN (10 mL, 1:1 v/v) under a nitrogen atmosphere. To this solution was added anhydrous $SnCl_2$ (0.65 g, 3.4 mmol, 16 equiv), and the reaction mixture was

stirred at rt in the dark for 20 h. A dark blue crude product was formed, which were collected by suction filtration and washed with a 1:1 mixture of THF/MeCN until the filtrate became colorless, and then dried under vacuum to afford compound **14** (0.12 g, 0.07 mmol, 27%) as a dark blue solid. m.p. 166.2 °C (decomp.). FTIR (neat): 3565, 2940, 2889, 2863, 2131, 1898, 1659, 1599, 1499, 1460, 1366, 1257, 1177, 1069, 1014, 994, 918, 879, 798, 741, 674, 585, 505, 459 cm^{-1}. HRMS (MALDI+, DCTB): m/z calcd. for $C_{120}H_{148}Si_6O_2$ $[M]^+$: 1789.00894, found: 1789.00786; correct isotope distribution.

3 NMR Spectra for New Compounds

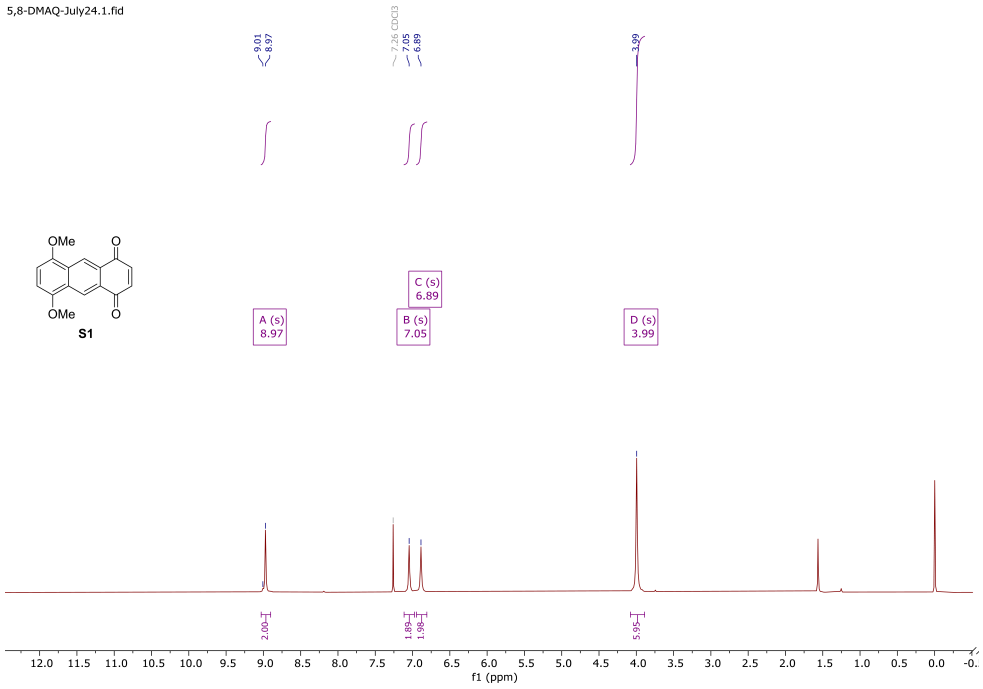

Figure S-4: ^{1}H NMR (300 Hz, $CDCl_3$) spectrum of compound **S1**.

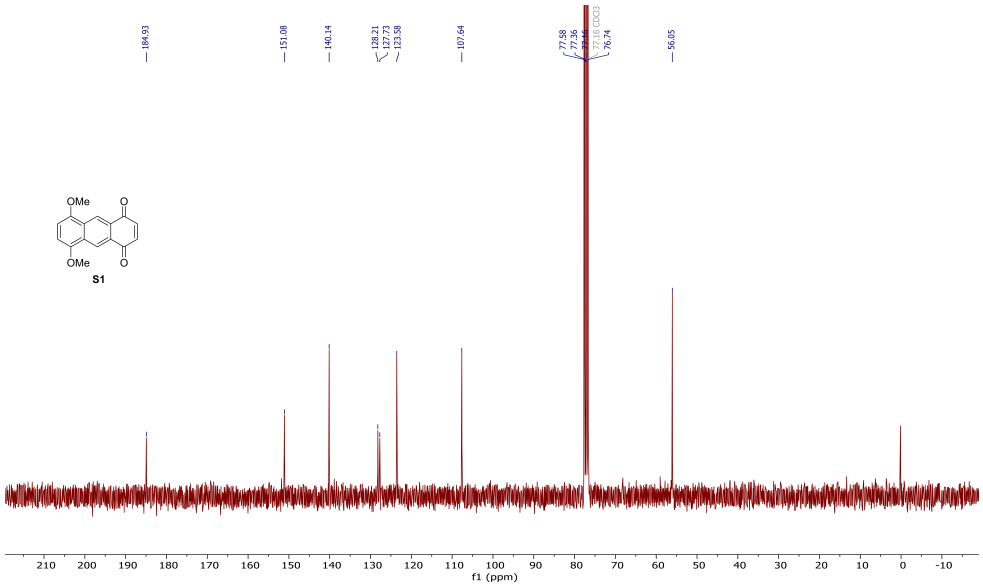

Figure S-5: $^{13}C\{^{1}H\}$ NMR (75 Hz, $CDCl_3$) spectrum of compound **S1**.

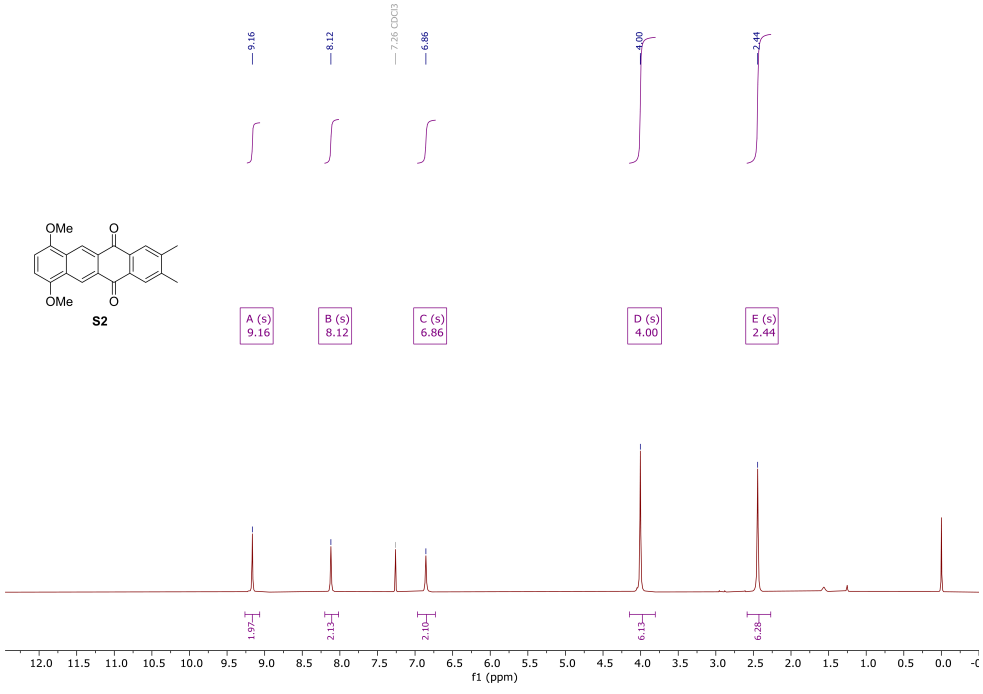

Figure S-6: ^{1}H NMR (300 Hz, $CDCl_3$) spectrum of compound **S2**.

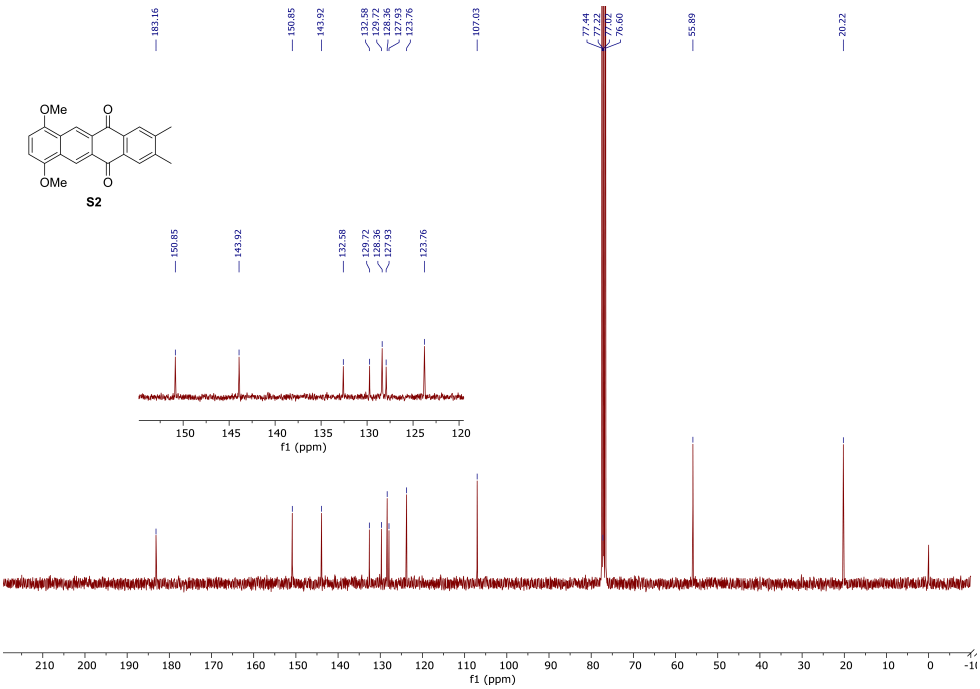

Figure S-7: $^{13}C\{^{1}H\}$ NMR (75 Hz, $CDCl_3$) spectrum of compound **S2**.

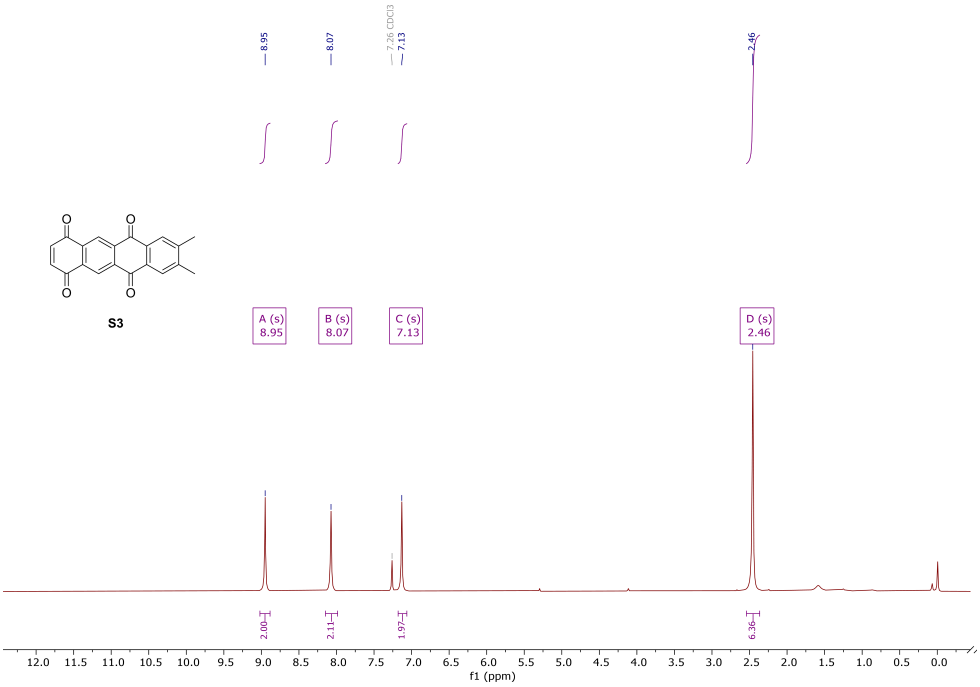

Figure S-8: ^{1}H NMR (300 Hz, $CDCl_3$) spectrum of compound **S3**.

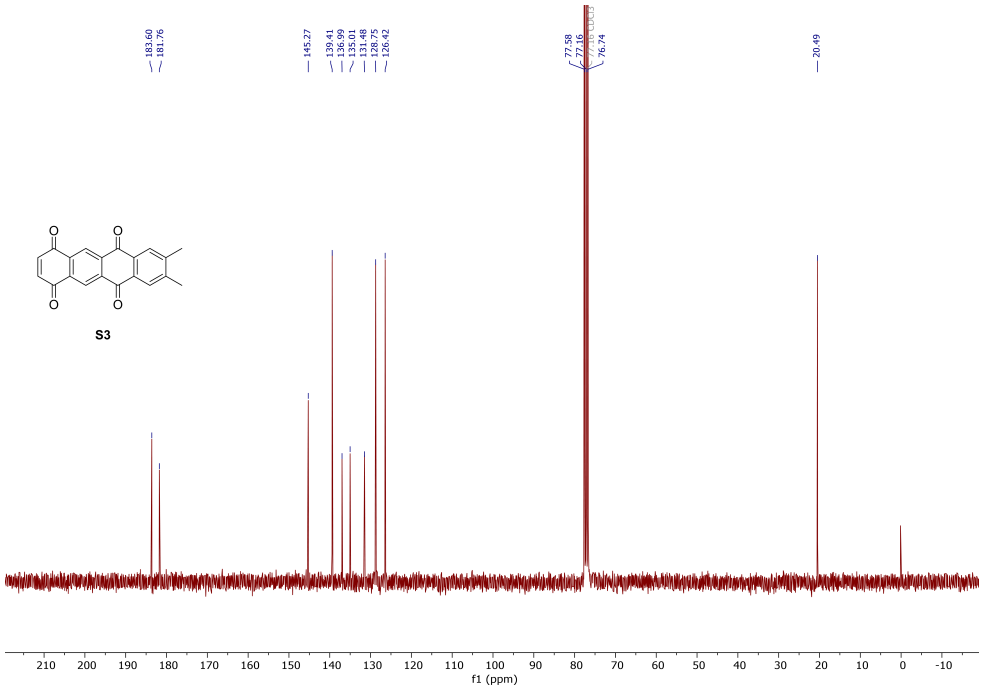

Figure S-9: $^{13}C\{^{1}H\}$ NMR (75 Hz, $CDCl_3$) spectrum of compound **S3**.

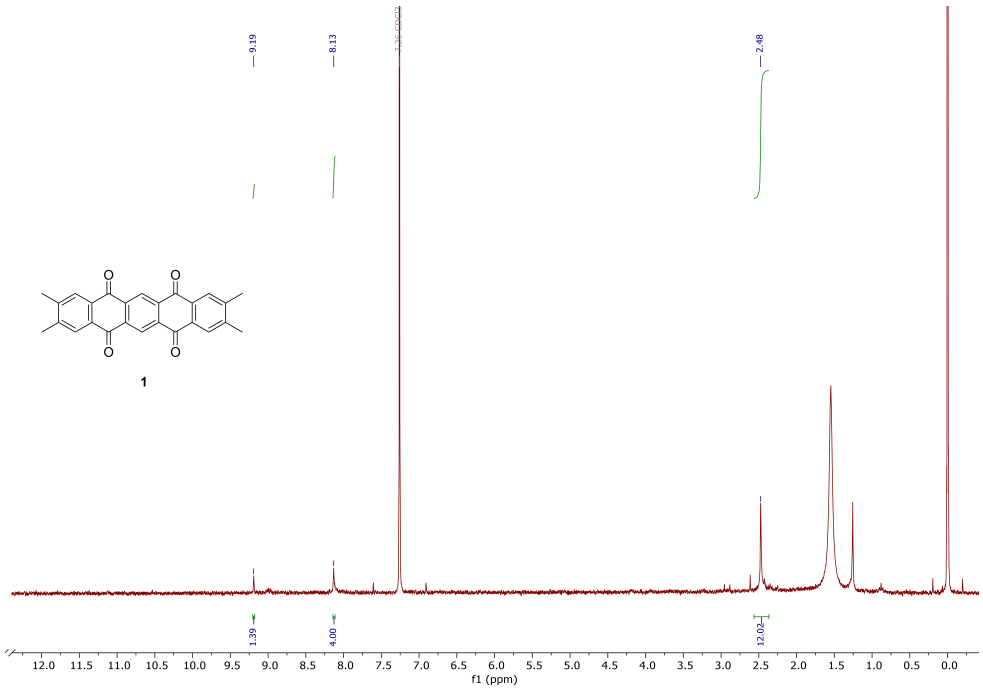

Figure S-10: ^{1}H NMR (300 Hz, $CDCl_3$) spectrum of compound **1**.

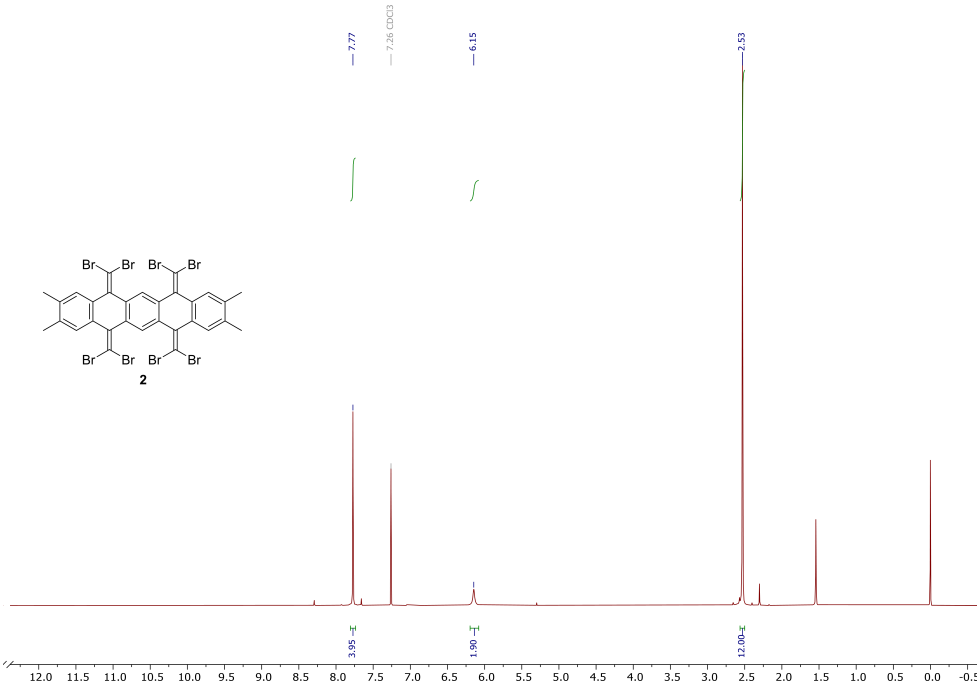

Figure S-11: ^{1}H NMR (300 Hz, $CDCl_3$) spectrum of compound **2**.

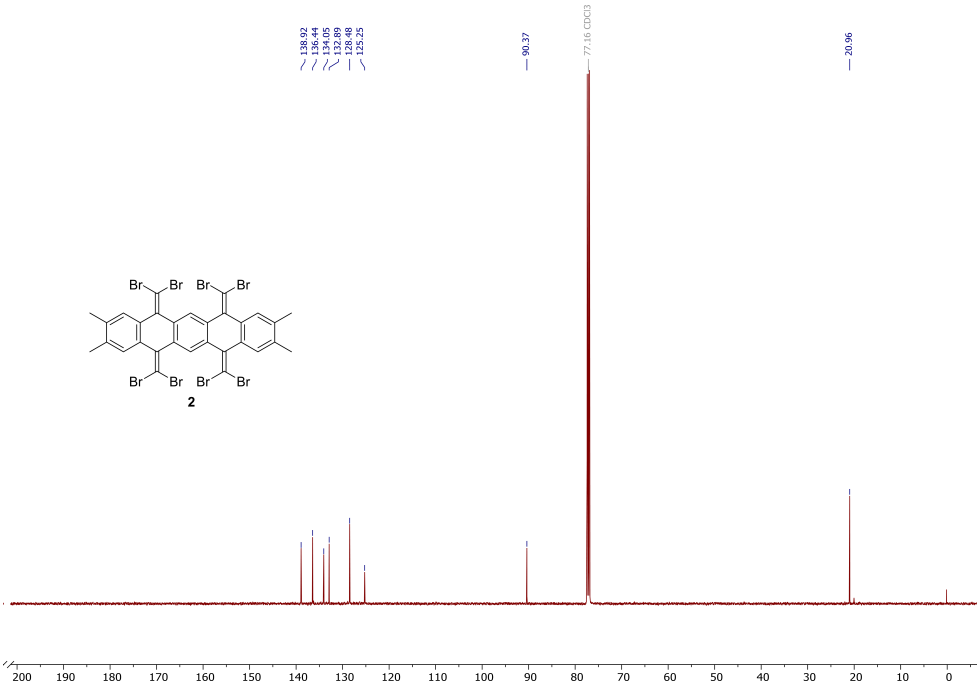

Figure S-12: $^{13}C\{^{1}H\}$ NMR (75 Hz, $CDCl_3$) spectrum of compound **2**.

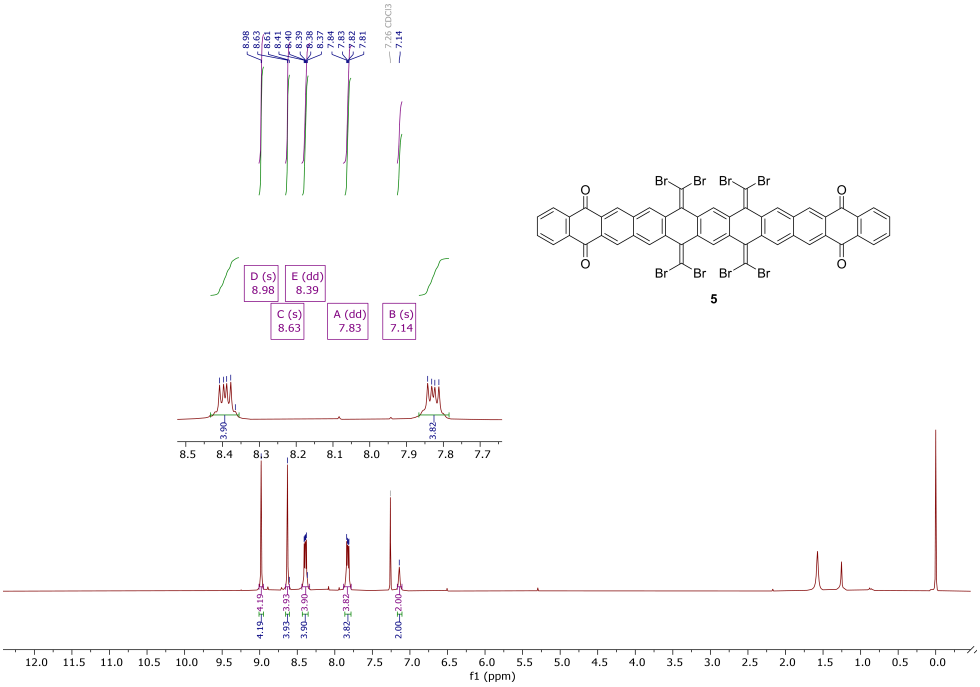

Figure S-13: ^{1}H NMR (300 Hz, $CDCl_3$) spectrum of compound **5**.

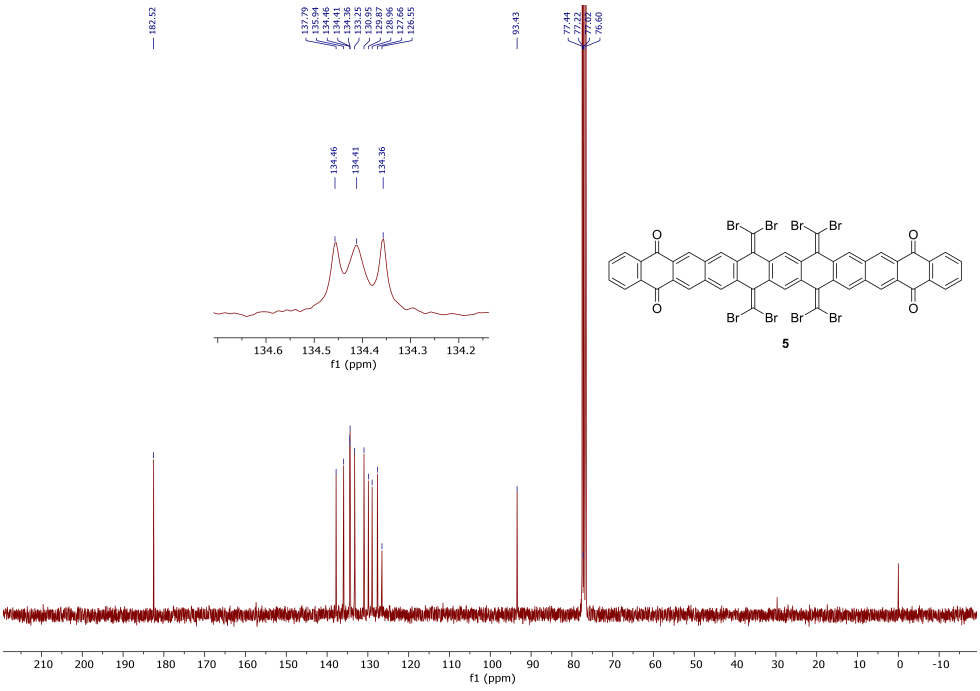

Figure S-14: $^{13}C\{^{1}H\}$ NMR (75 Hz, $CDCl_3$) spectrum of compound **5**.

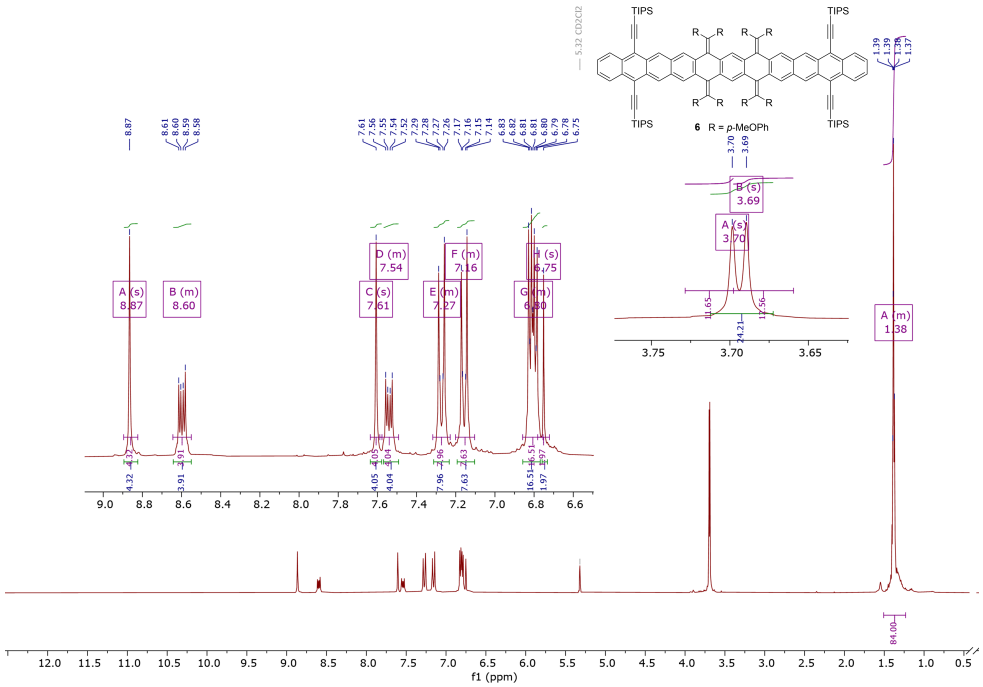

Figure S-15: ^{1}H NMR (300 Hz, CD_2Cl_2) spectrum of compound **6**.

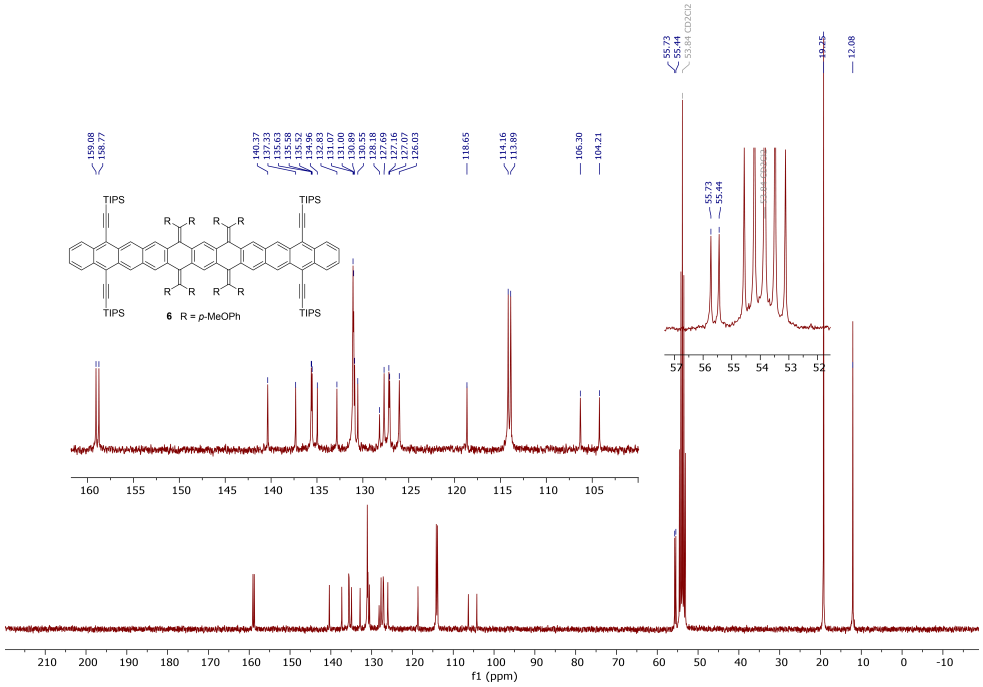

Figure S-16: ^{13}C{^{1}H} NMR (75 Hz, CD_2Cl_2) spectrum of compound **6**.

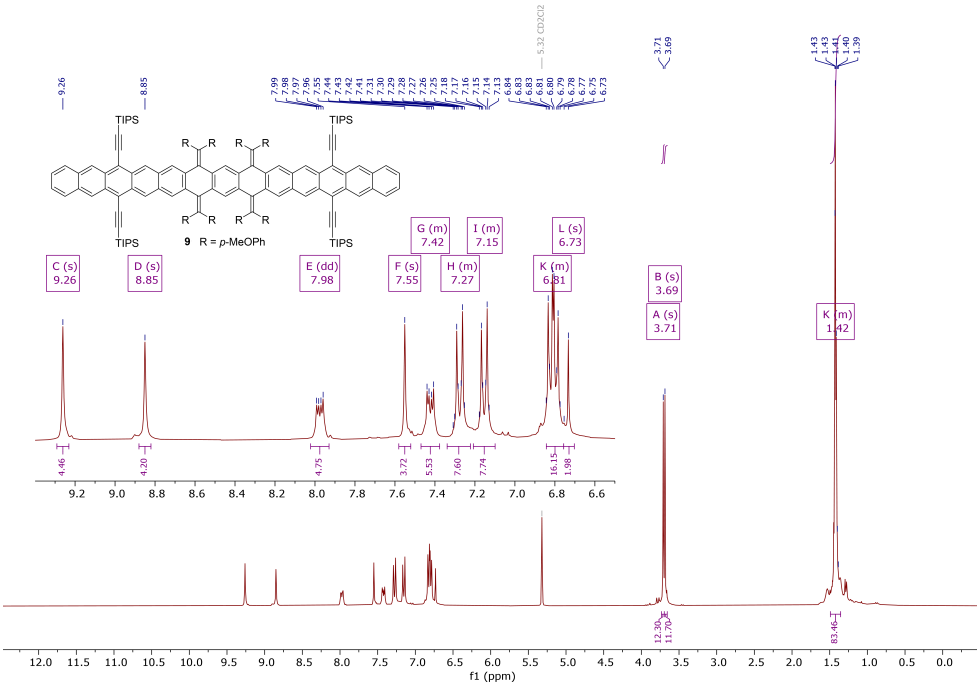

Figure S-17: ^{1}H NMR (300 Hz, CD_2Cl_2) spectrum of compound **9**.

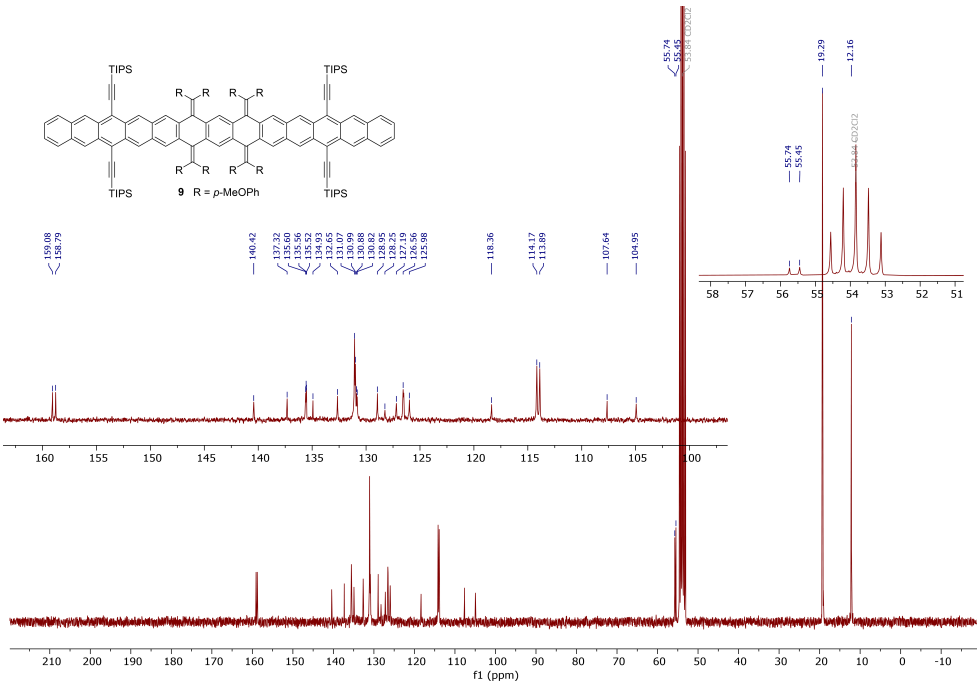

Figure S-18: ^{13}C{^{1}H} NMR (75 Hz, CD_2Cl_2) spectrum of compound **9**.

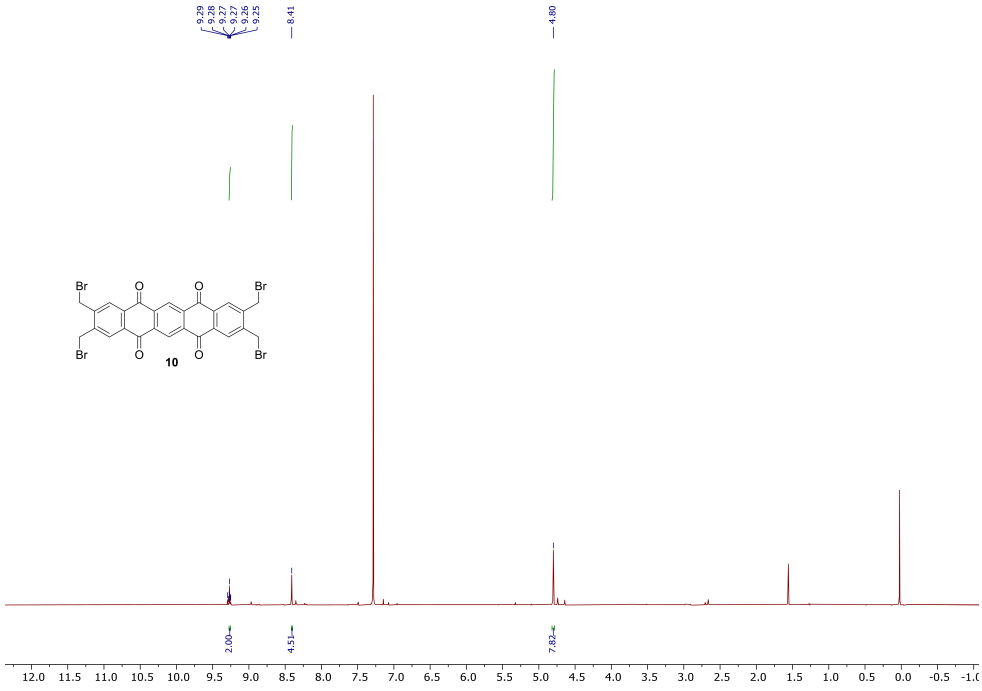

Figure S-19: ^{1}H NMR (300 Hz, $CDCl_3$) spectrum of compound **10**.

4 IR Spectra for New Compounds

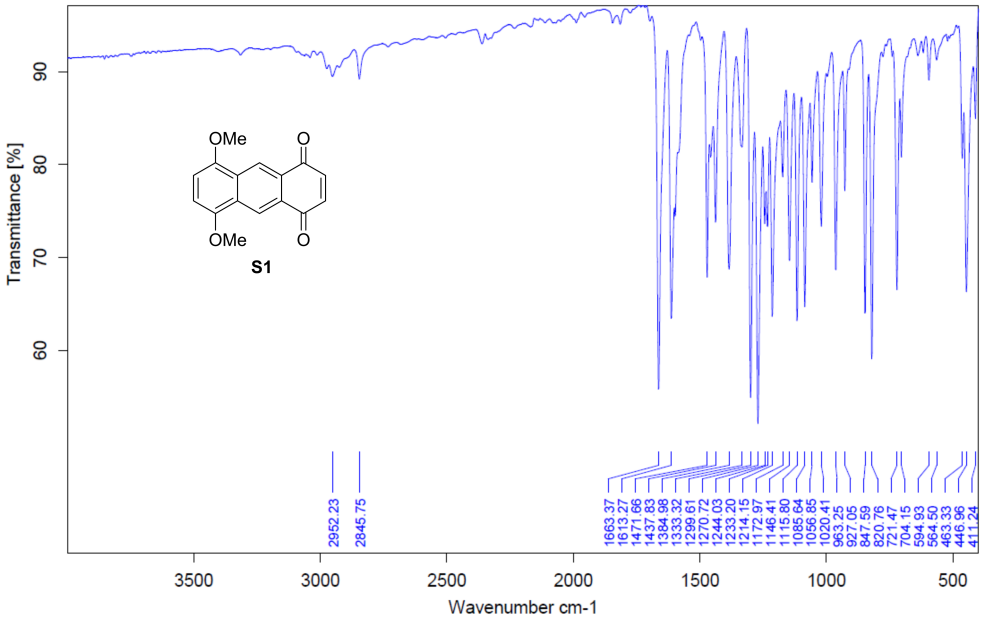

Figure S-20: IR spectrum of compound **S1**.

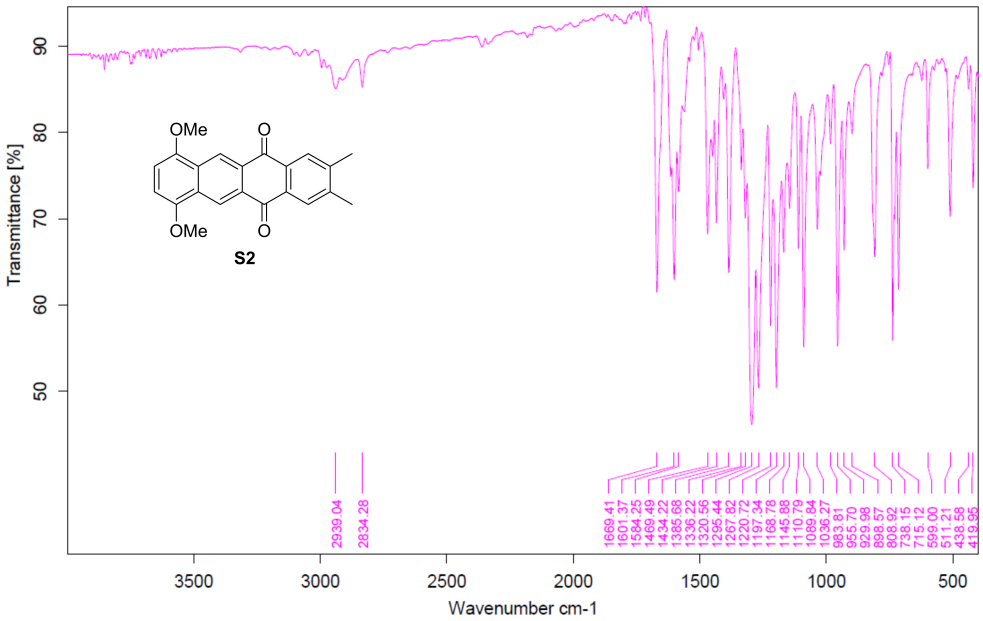

Figure S-21: IR spectrum of compound **S2**.

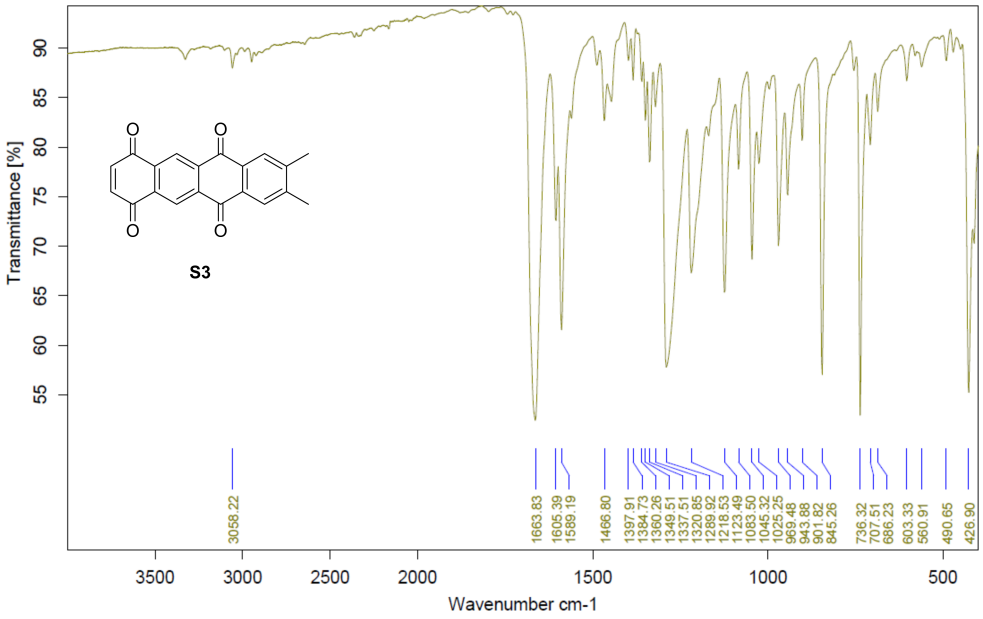

Figure S-22: IR spectrum of compound **S3**.

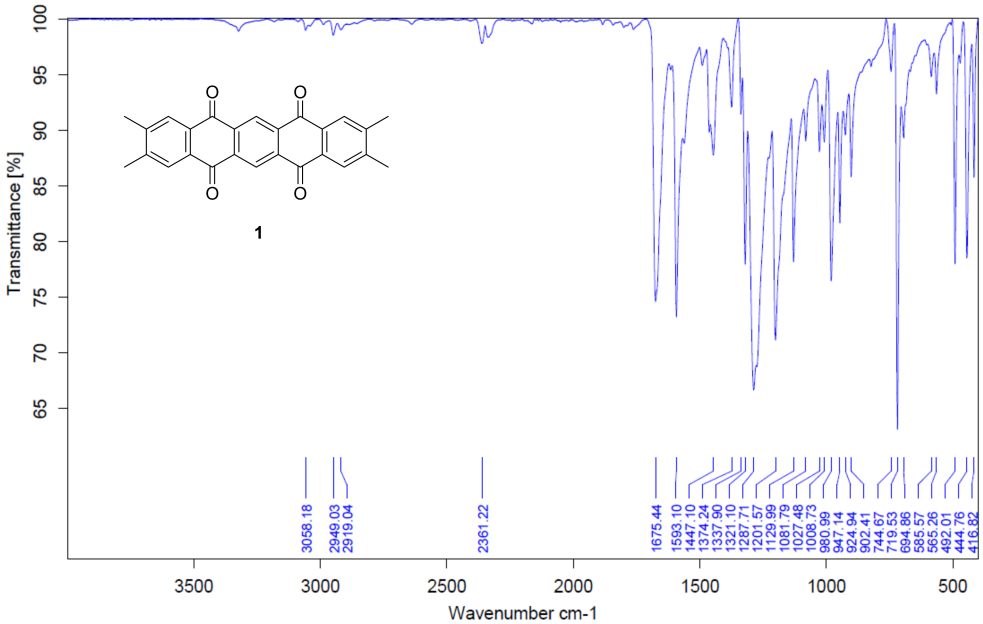

Figure S-23: IR spectrum of compound **1**.

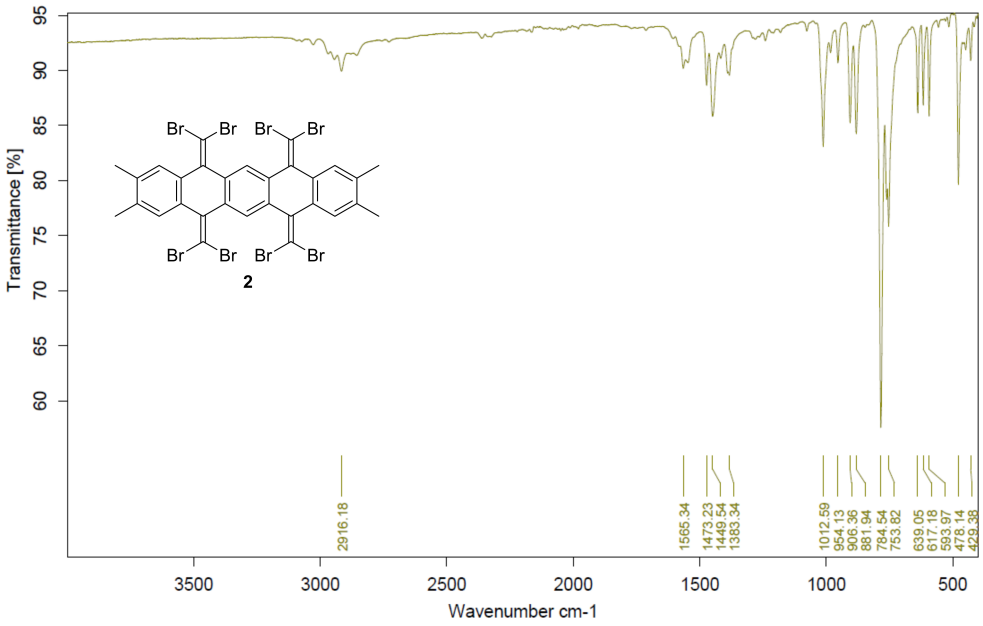

Figure S-24: IR spectrum of compound **2**.

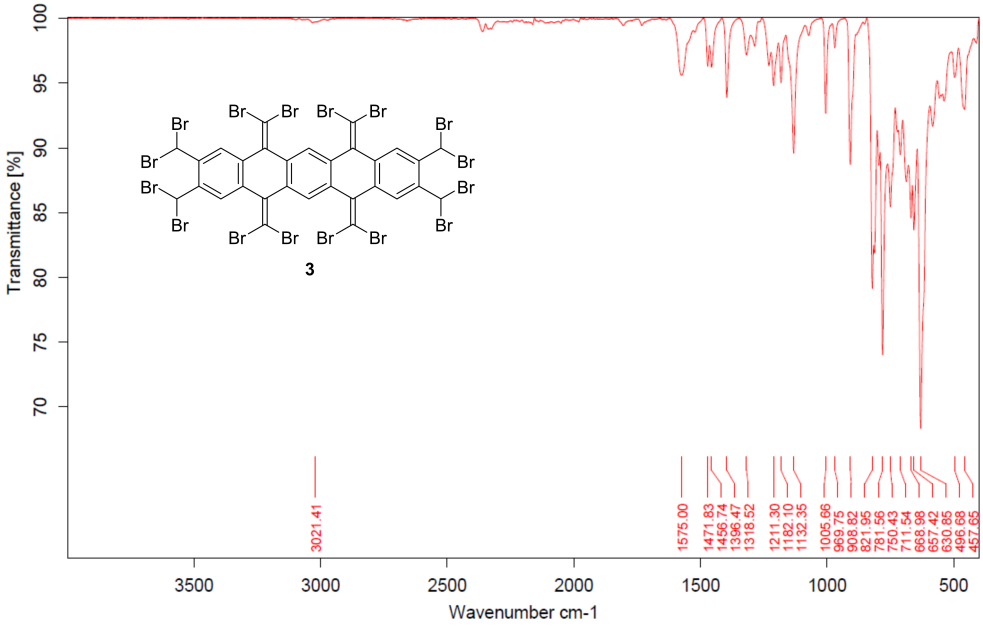

Figure S-25: IR spectrum of compound **3**.

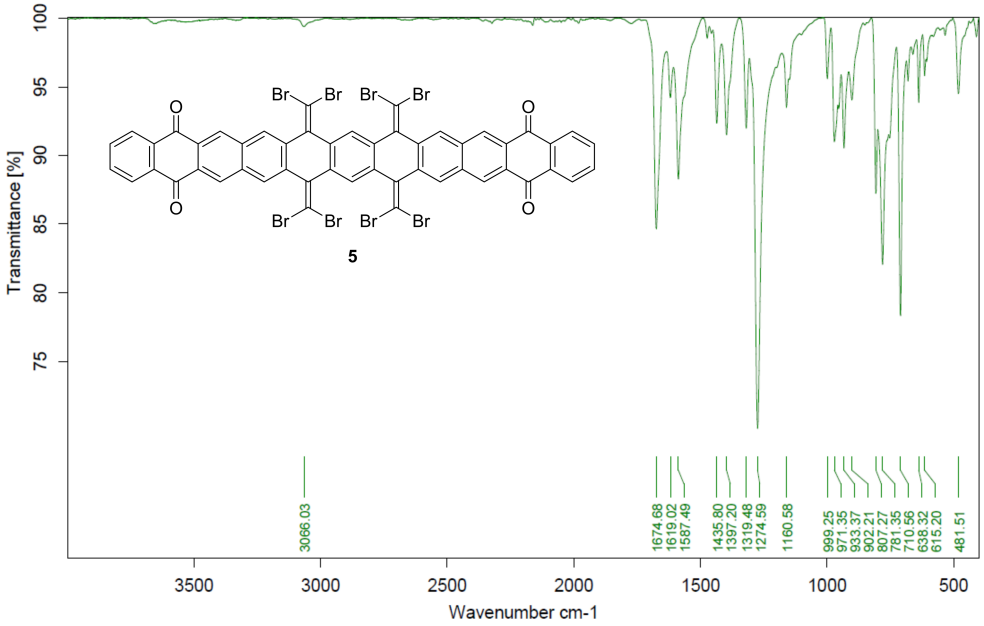

Figure S-26: IR spectrum of compound **5**.

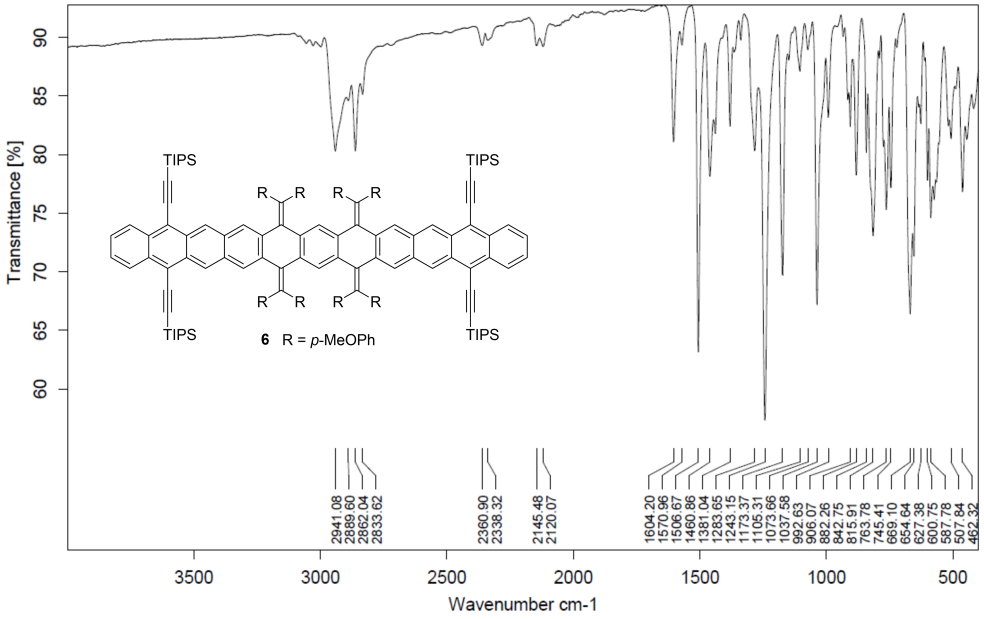

Figure S-27: IR spectrum of compound **6**.

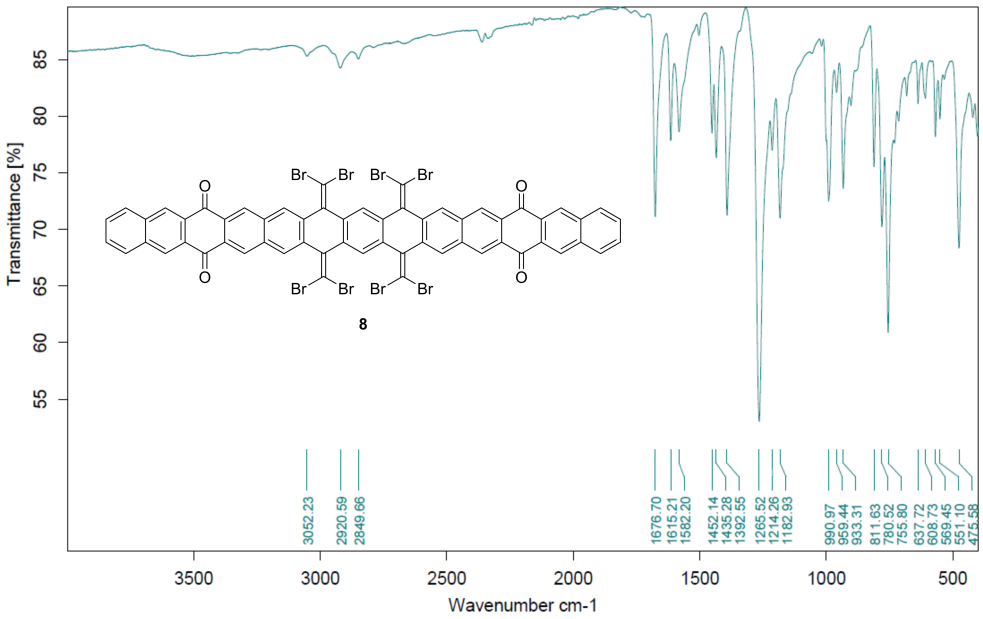

Figure S-28: IR spectrum of compound **8**.

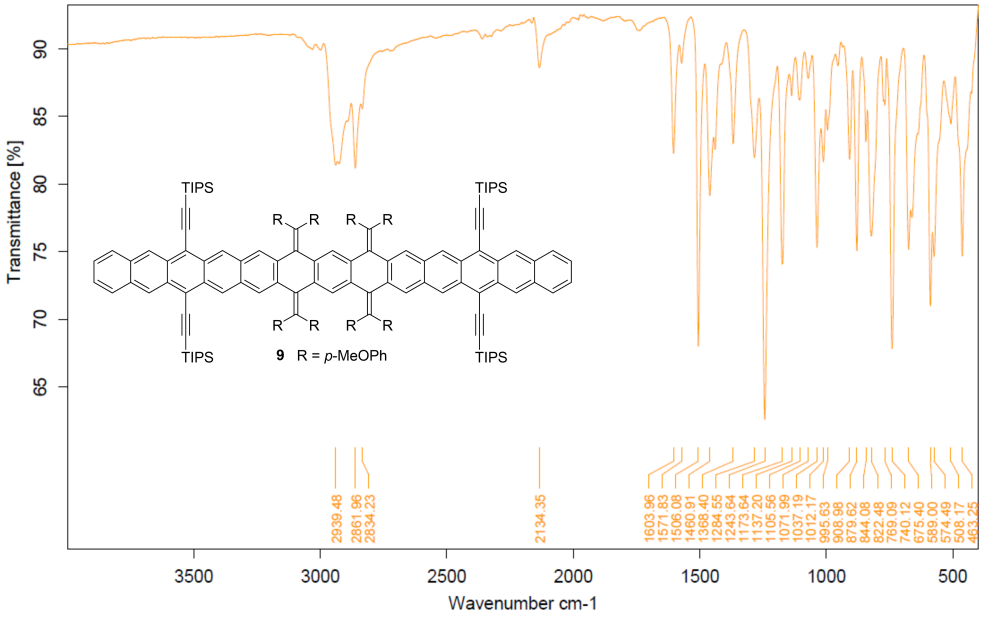

Figure S-29: IR spectrum of compound **9**.

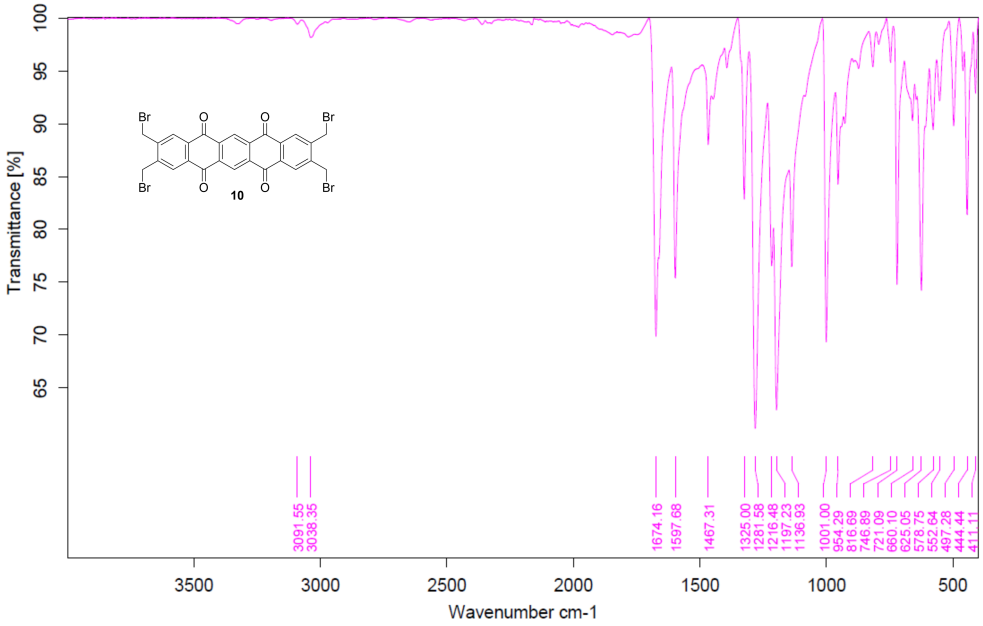

Figure S-30: IR spectrum of compound **10**.

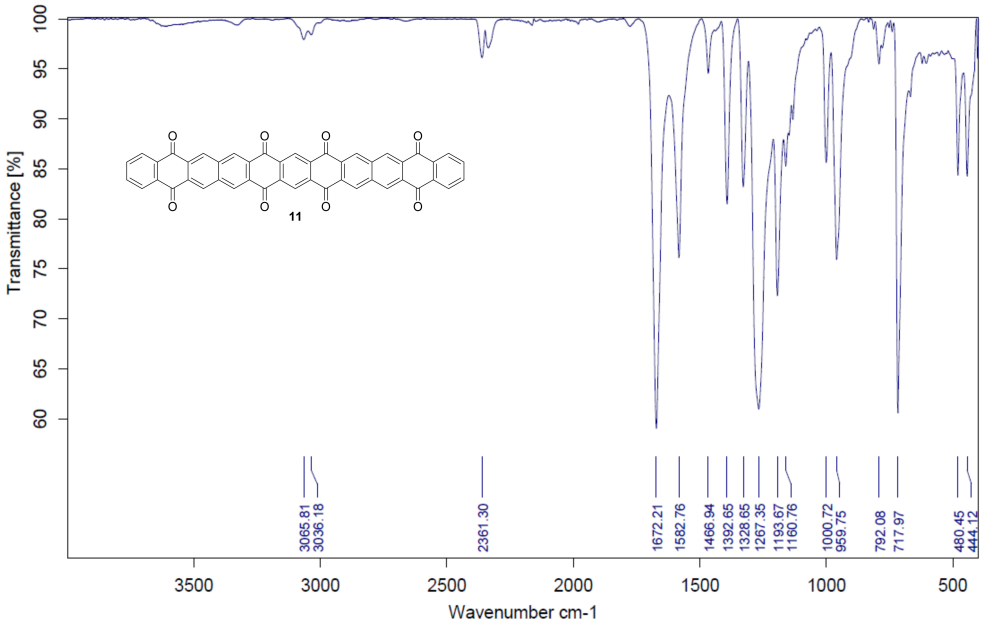

Figure S-31: IR spectrum of compound **11**.

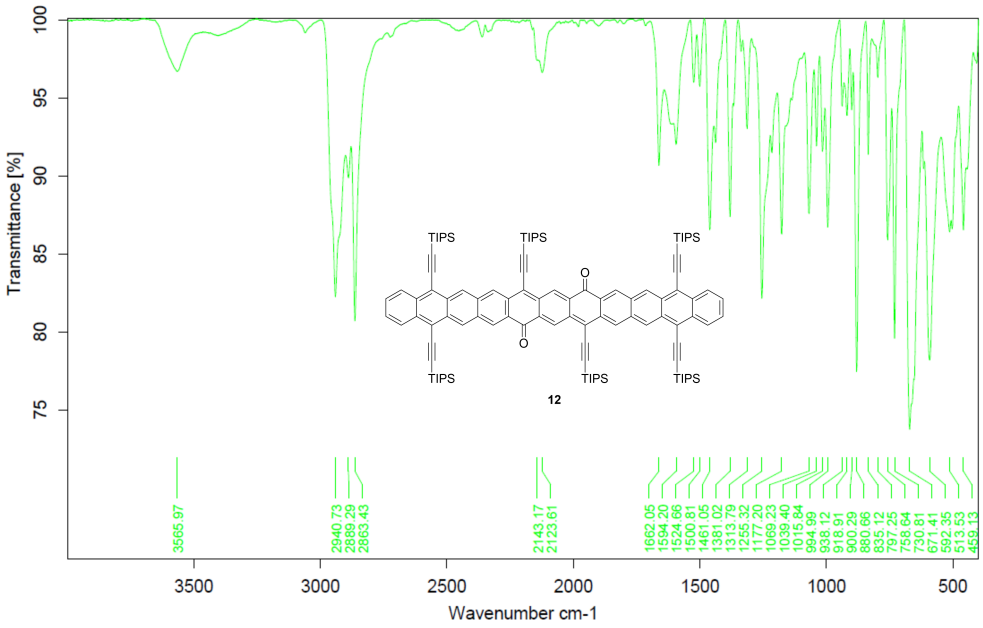

Figure S-32: IR spectrum of compound **12**.

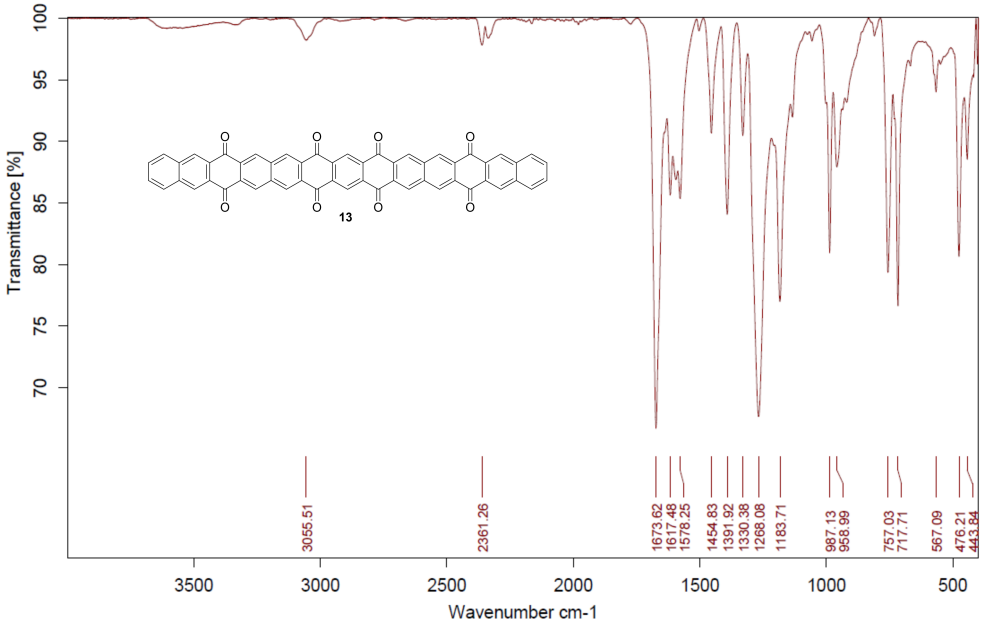

Figure S-33: IR spectrum of compound **13**.

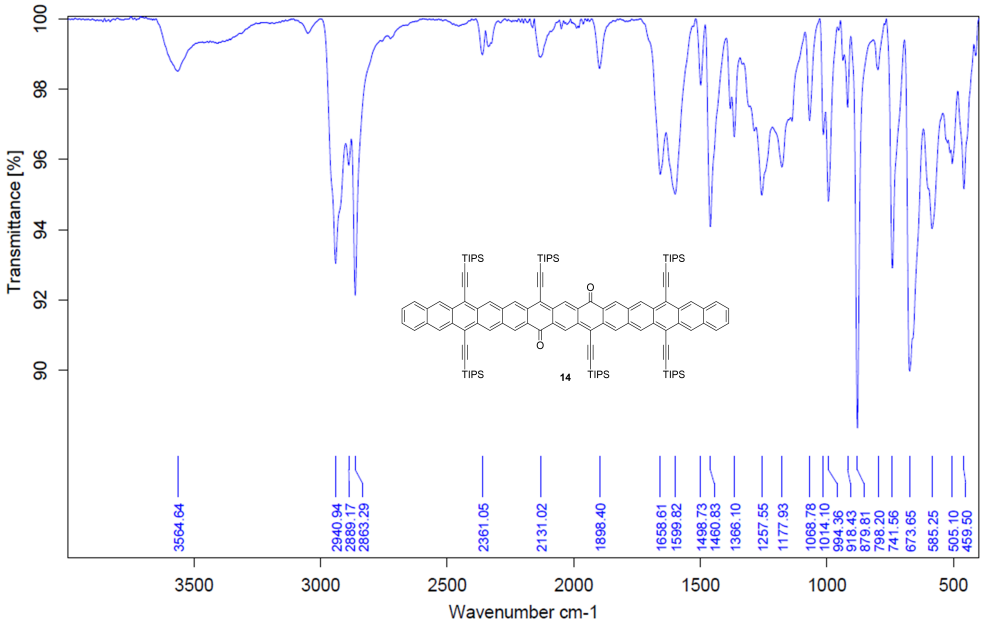

Figure S-34: IR spectrum of compound **14**.

5 MALDI-TOF Mass Spectra

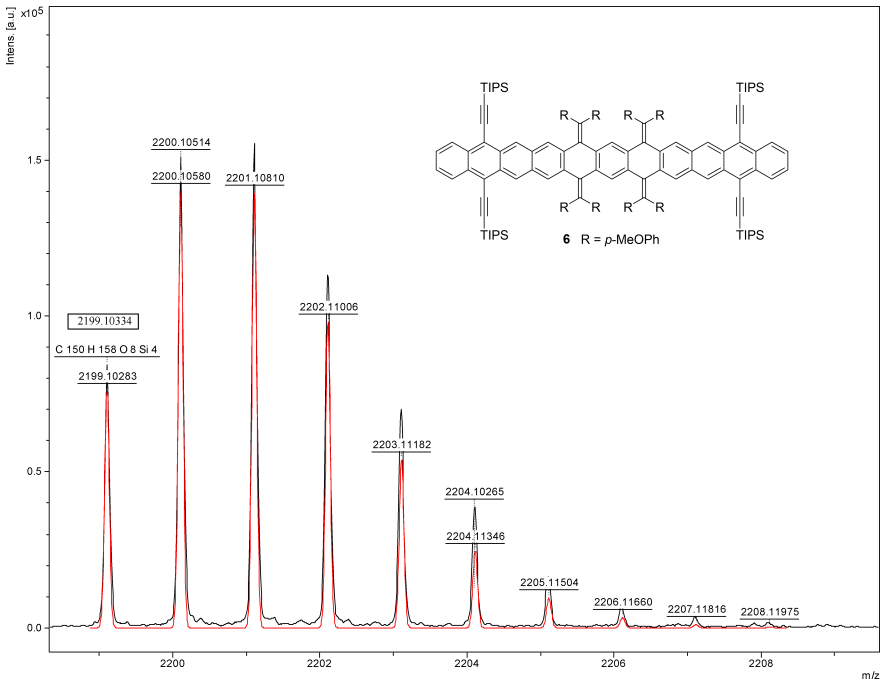

Figure S-35: Experimentally observed (blue trace) and theoretically calculated (red trace) isotope distribution patterns for the molecular ion of **6**.

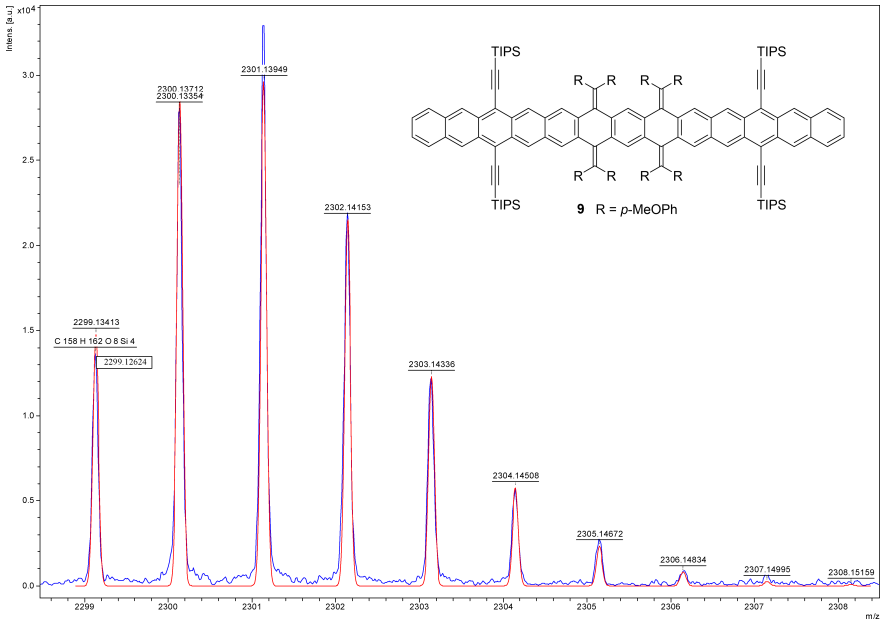

Figure S-36: Experimentally observed (blue trace) and theoretically calculated (red trace) isotope distribution patterns for the molecular ion of **9**.

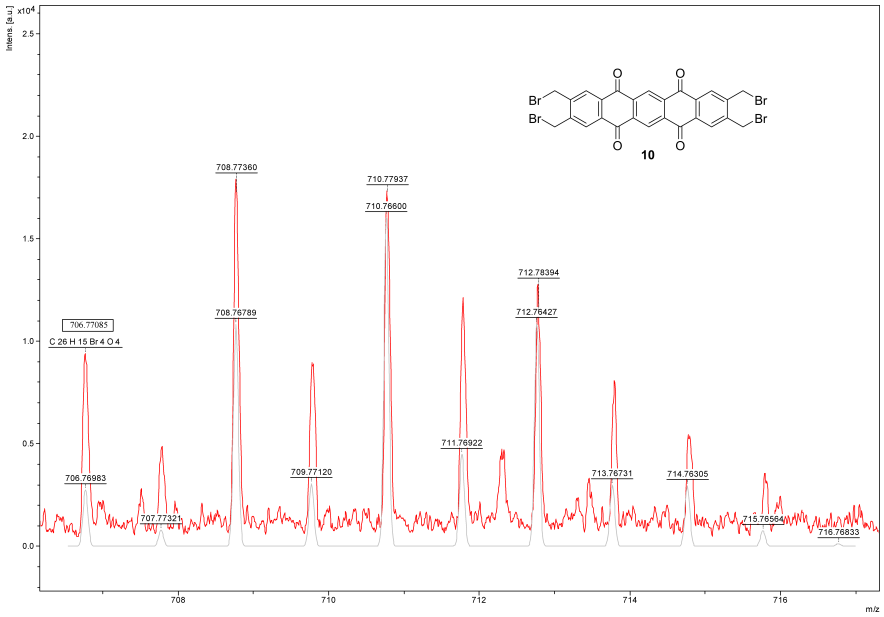

Figure S-37: Experimentally observed (blue trace) and theoretically calculated (red trace) isotope distribution patterns for the molecular ion of **10**.

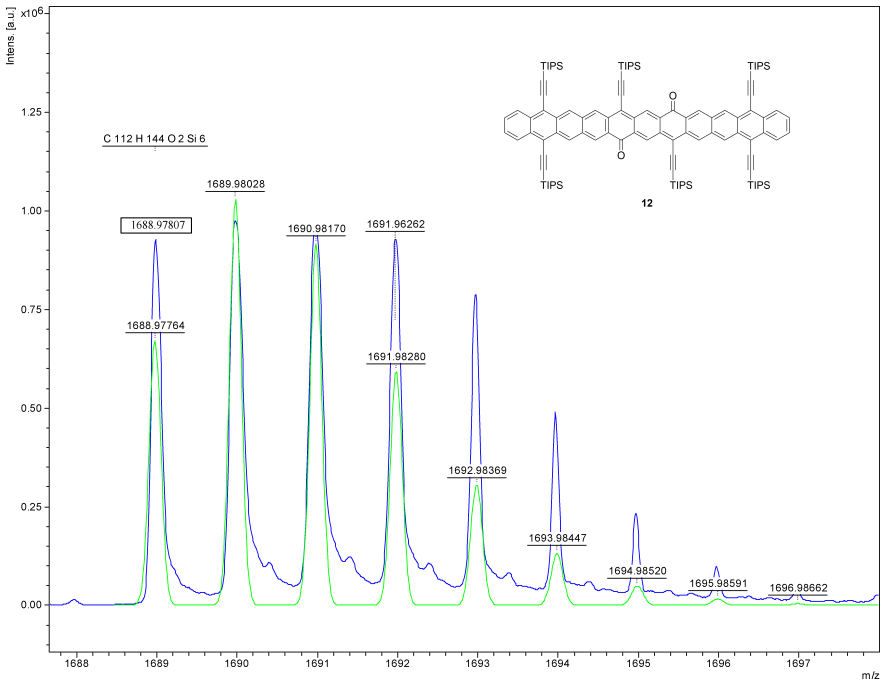

Figure S-38: Experimentally observed (blue trace) and theoretically calculated (green trace) isotope distribution patterns for the molecular ion of **12**.

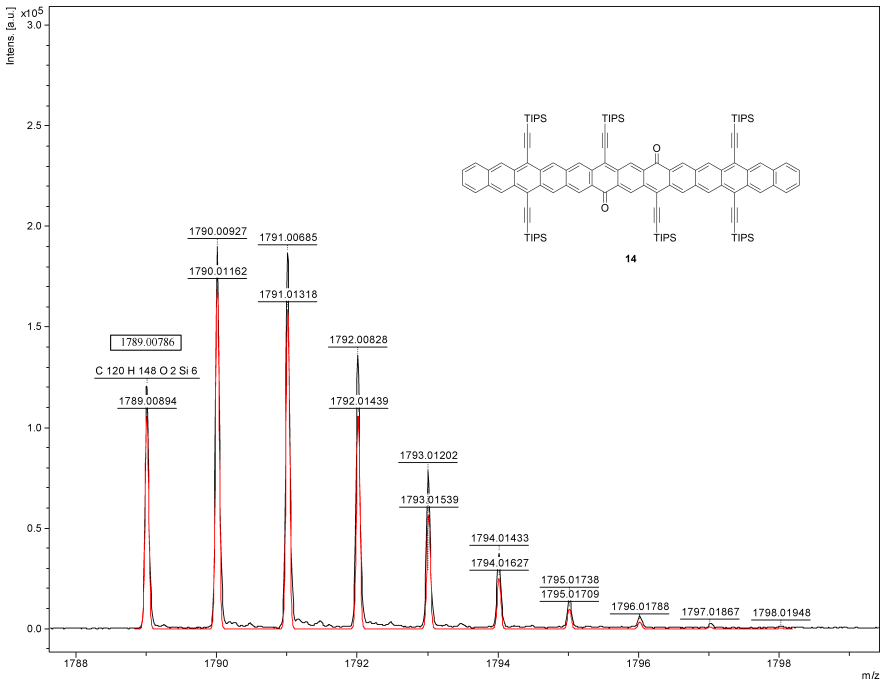

Figure S-39: Experimentally observed (blue trace) and theoretically calculated (green trace) isotope distribution patterns for the molecular ion of **14**.

6 X-ray Single Crystallographic Data

Table S-1: Crystal data and structure refinement of **2** (CCDC 2411812)

Empirical formula	$C_{30}H_{18}Br_8$
Formula weight	2035.45
Temperature (K)	100(2)
Crystal system	triclinic
Space group	P-*1*
a (Å)	13.8214(2)
b (Å)	17.5800(3)
c (Å)	18.4580(4)
α (°)	64.740(2)
β (°)	76.738(2)
γ (°)	73.036(2)
Volume (Å^3)	3850.97(14)
Z	4
ρ_{calc} (g/cm^3)	1.755
μ (mm^{-1})	10.087
F(000)	1912.0
Crystal size (mm^3)	0.134 × 0.029 × 0.023
Radiation	Cu Kα (λ = 1.54184 Å)
2θ range for data collection (°)	5.334 to 155.712
Index ranges	$-16 \leq h \leq 17$, $-22 \leq k \leq 22$, $-23 \leq l \leq 23$
Reflections collected	97212
Independent reflections	16120 [R_{int} = 0.0770, R_σ = 0.0502]
Data/restraints/parameters	16120/0/693
Goodness-of-fit on F^2	1.052
Final R indexes [I≥2σ(I)]	R_1 = 0.0527, wR_2 = 0.1418
Final R indexes [all data]	R_1 = 0.0624, wR_2 = 0.1477
Largest diff. peak/hole (e Å^{-3})	1.09 / −0.88

Table S-2: Crystal data and structure refinement of **3** (CCDC 2411813)

Empirical formula	$C_{30}H_{10}Br_{16}$
Formula weight	1648.94
Temperature (K)	100(2)
Crystal system	triclinic
Space group	P-*1*
a (Å)	9.0954(3)
b (Å)	14.4051(4)
c (Å)	15.0563(6)
α (°)	94.689(3)
β (°)	92.366(3)
γ (°)	101.513(3)
Volume (Å^3)	1923.15(12)
Z	2
ρ_{calc} (g/cm^3)	2.848
μ (mm^{-1})	19.916
F(000)	1500.0
Crystal size (mm^3)	0.078 × 0.036 × 0.026
Radiation	Cu Kα (λ = 1.54184 Å)
2θ range for data collection (°)	5.9 to 155.11
Index ranges	$-11 \leq h \leq 11$, $-18 \leq k \leq 17$, $-18 \leq l \leq 18$
Reflections collected	39761
Independent reflections	8012 [R_{int} = 0.0672, R_σ = 0.0507]
Data/restraints/parameters	8012/51/497
Goodness-of-fit on F^2	1.059
Final R indexes [I≥2σ(I)]	R_1 = 0.0639, wR_2 = 0.1588
Final R indexes [all data]	R_1 = 0.0798, wR_2 = 0.1683
Largest diff. peak/hole (e Å^{-3})	1.67 / −2.36

Table S-3: Crystal data and structure refinement of **5** (CCDC 2411822)

Empirical formula	$C_{62.5}H_{55.5}Br_8O_{10.25}S_{6.25}$
Formula weight	1810.22
Temperature (K)	100(2)
Crystal system	monoclinic
Space group	$P2_1/n$
a (Å)	14.1360(2)
b (Å)	31.3361(5)
c (Å)	31.0794(5)
β (°)	101.780(2)
Volume (Å^3)	13477.2(4)
Z	8
ρ_{calc} (g/cm^3)	1.784
μ (mm^{-1})	7.968
F(000)	7140.0
Crystal size (mm^3)	0.132 × 0.062 × 0.056
Radiation	Cu Kα (λ = 1.54184 Å)
2θ range for data collection (°)	5.64 to 159.154
Index ranges	$-17 \leq h \leq 17$, $-39 \leq k \leq 39$, $-39 \leq l \leq 39$
Reflections collected	40129
Independent reflections	40129 [R_σ = 0.0356]
Data/restraints/parameters	40129/12/1663
Goodness-of-fit on F^2	1.019
Final R indexes [I≥2σ(I)]	R_1 = 0.0822, wR_2 = 0.2118
Final R indexes [all data]	R_1 = 0.1099, wR_2 = 0.2347
Largest diff. peak/hole (e Å^{-3})	1.72 / −1.27

Table S-4: Crystal data and structure refinement of **6** (CCDC 2411817)

Empirical formula	$C_{153.69}H_{166.61}O_8Si_4$
Formula weight	2254.12
Temperature (K)	100(2)
Crystal system	triclinic
Space group	P-*1*
a (Å)	14.5849(3)
b (Å)	16.5478(3)
c (Å)	17.0332(3)
α (°)	61.390(2)
β (°)	66.698(2)
γ (°)	85.0400(10)
Volume (Å^3)	3287.47(13)
Z	1
ρ_{calc} (g/cm^3)	1.139
μ (mm^{-1})	0.859
F(000)	1209.0
Crystal size (mm^3)	0.121 × 0.039 × 0.036
Radiation	Cu Kα (λ = 1.54184 Å)
2θ range for data collection (°)	6.134 to 159.252
Index ranges	$-18 \leq h \leq 18$, $-19 \leq k \leq 21$, $-20 \leq l \leq 21$
Reflections collected	82699
Independent reflections	14060 [R_{int} = 0.0537, R_σ = 0.0355]
Data/restraints/parameters	14060/0/780
Goodness-of-fit on F^2	1.018
Final R indexes [I≥2σ(I)]	R_1 = 0.0865, wR_2 = 0.2463
Final R indexes [all data]	R_1 = 0.1035, wR_2 = 0.2654
Largest diff. peak/hole (e Å^{-3})	1.11 / −0.71

Table S-5: Crystal data and structure refinement of **9** (CCDC 2411821)

Empirical formula	$C_{158}H_{162}O_8Si_4$
Formula weight	2301.23
Temperature (K)	100(2)
Crystal system	triclinic
Space group	P-*1*
a (Å)	16.1835(4)
b (Å)	16.2998(4)
c (Å)	16.9540(4)
α (°)	62.248(2)
β (°)	66.626(2)
γ (°)	89.796(2)
Volume (Å^3)	3541.51(17)
Z	1
ρ_{calc} (g/cm^3)	1.079
μ (mm^{-1})	0.808
F(000)	1230.0
Crystal size (mm^3)	0.028 × 0.022 × 0.015
Radiation	Cu Kα (λ = 1.54184 Å)
2θ range for data collection (°)	6.104 to 159.12
Index ranges	$-20 \leq h \leq 19$, $-20 \leq k \leq 20$, $-21 \leq l \leq 21$
Reflections collected	72260
Independent reflections	15076 [R_{int} = 0.0471, R_σ = 0.0347]
Data/restraints/parameters	15076/0/793
Goodness-of-fit on F^2	1.063
Final R indexes [I≥2σ(I)]	R_1 = 0.0600, wR_2 = 0.1648
Final R indexes [all data]	R_1 = 0.0763, wR_2 = 0.1795
Largest diff. peak/hole (e Å^{-3})	1.27 / −0.57

Table S-6: Crystal data and structure refinement of **12** (CCDC 2428575)

Empirical formula	$C_{114.89}H_{146.41}Cl_{0.48}O_2Si_6$
Formula weight	1745.96
Temperature (K)	100(2)
Crystal system	monoclinic
Space group	C2/c
a (Å)	53.8990(6)
b (Å)	14.6150(2)
c (Å)	14.74620(10)
α (°)	90
β (°)	97.4070(10)
γ (°)	90
Volume (Å^3)	11519.1(2)
Z	4
ρ_{calc} (g/cm^3)	1.006
μ (mm^{-1})	1.106
F(000)	3776.0
Crystal size (mm^3)	0.13 × 0.102 × 0.084
Radiation	Cu Kα (λ = 1.54184 Å)
2θ range for data collection (°)	6.27 to 158.742
Index ranges	$-68 \leq h \leq 67$, $-18 \leq k \leq 18$, $-18 \leq l \leq 16$
Reflections collected	75165
Independent reflections	12302 [R_{int} = 0.0370, R_σ = 0.0276]
Data/restraints/parameters	12302/158/920
Goodness-of-fit on F^2	1.491
Final R indexes [I≥2σ(I)]	R_1 = 0.1096, wR_2 = 0.3392
Final R indexes [all data]	R_1 = 0.1313, wR_2 = 0.3706
Largest diff. peak/hole (e Å^{-3})	0.79 / −0.33

Table S-7: Crystal data and structure refinement of **14** (CCDC 2428580)

Empirical formula	$C_{126.63}H_{153.72}Cl_{0.24}O_2Si_6$
Formula weight	1884.82
Temperature (K)	100(2)
Crystal system	triclinic
Space group	$P\bar{1}$
a (Å)	10.4872(3)
b (Å)	10.9114(3)
c (Å)	27.8018(7)
α (°)	89.132(2)
β (°)	81.149(2)
γ (°)	66.763(2)
Volume (Å^3)	2884.84(14)
Z	1
ρ_{calc} (g/cm^3)	1.085
μ (mm^{-1})	1.089
F(000)	1018.0
Crystal size (mm^3)	0.105 × 0.044 × 0.026
Radiation	Cu Kα (λ = 1.54184 Å)
2θ range for data collection (°)	6.444 to 159.414
Index ranges	$-13 \leq h \leq 13$, $-13 \leq k \leq 13$, $-34 \leq l \leq 35$
Reflections collected	59788
Independent reflections	12305 [R_{int} = 0.0477, R_σ = 0.0363]
Data/restraints/parameters	12305/220/887
Goodness-of-fit on F^2	1.029
Final R indexes [I≥2σ(I)]	R_1 = 0.0976, wR_2 = 0.2817
Final R indexes [all data]	R_1 = 0.1223, wR_2 = 0.3098
Largest diff. peak/hole (e Å^{-3})	1.21 / −0.72

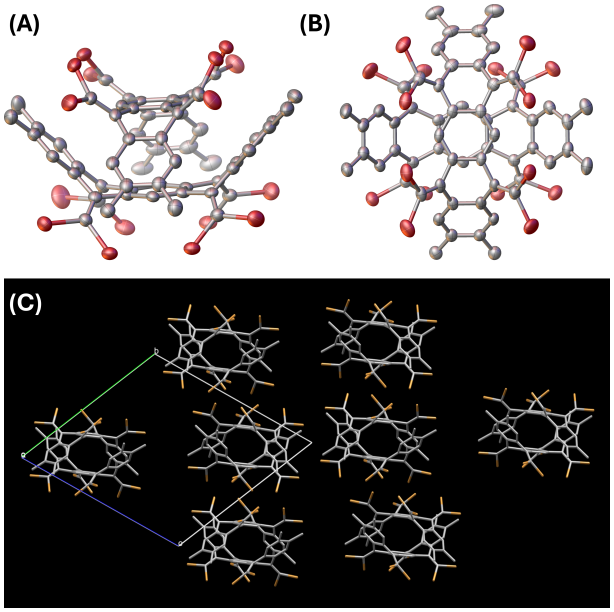

Figure S-40: (A) and (B): ORTEP drawings (50% ellipsoid probability) of a dimeric assembly of **2** viewed from different perspectives. (C): Crystal packing diagram of **2** viewed along the *a*-axis of the unit cell. Hydrogen atoms are omitted for clarity.

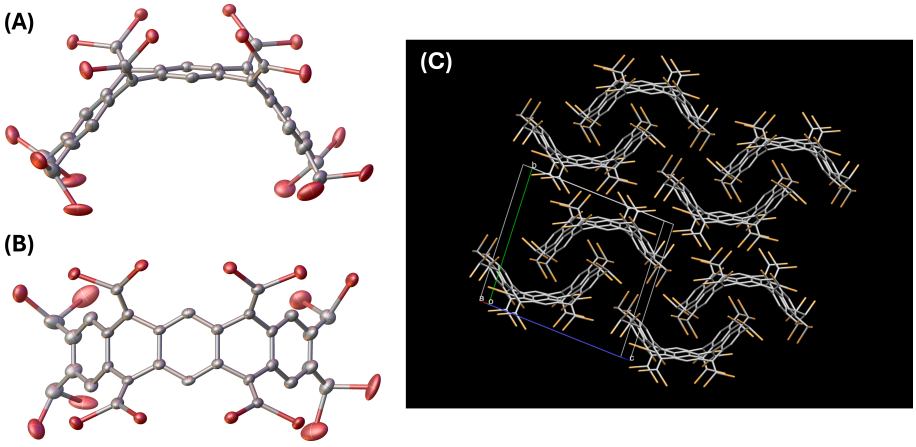

Figure S-41: (A) and (B): ORTEP drawings (50% ellipsoid probability) of **3** viewed from different perspectives. (C): Crystal packing diagram of **3** viewed along the *a*-axis of the unit cell. Hydrogen atoms are omitted for clarity.

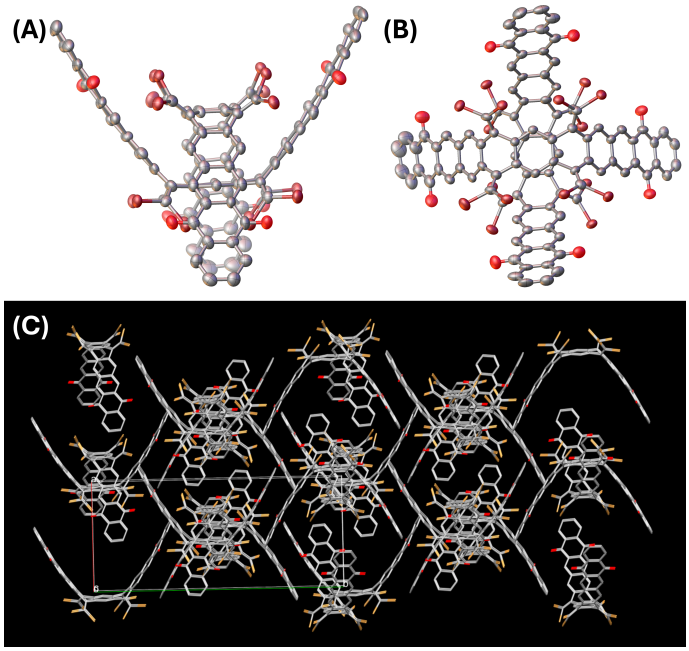

Figure S-42: (A) and (B): ORTEP drawings (50% ellipsoid probability) of a dimeric assembly of **5** viewed from different perspectives. (C): Crystal packing diagram of **5** viewed along the *c*-axis of the unit cell. Hydrogen atoms are omitted for clarity.

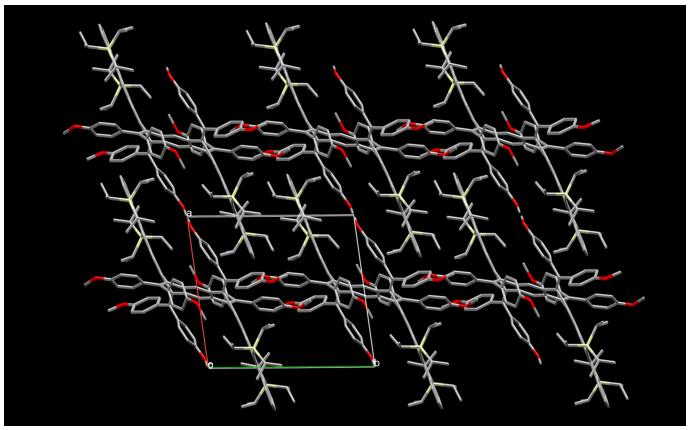

Figure S-43: Crystal packing diagram of **6** viewed along the *c*-axis of the unit cell. Hydrogen atoms are omitted for clarity.

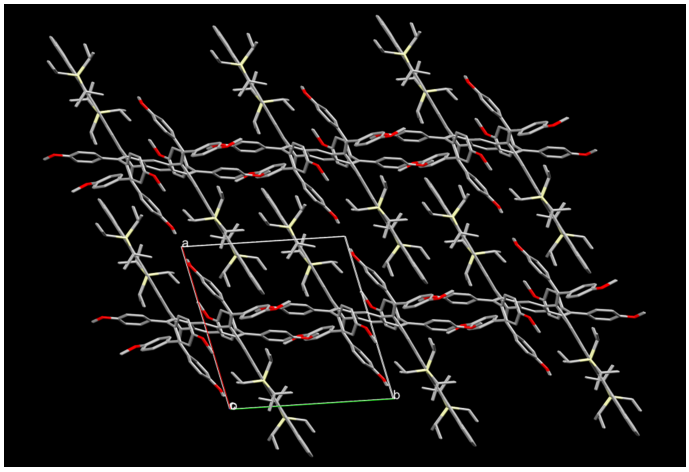

Figure S-44: Crystal packing diagram of **9** viewed along the *c*-axis of the unit cell. Hydrogen atoms are omitted for clarity.

7 Time-dependent UV-Vis-NIR Analysis of Cationic 6 and 9

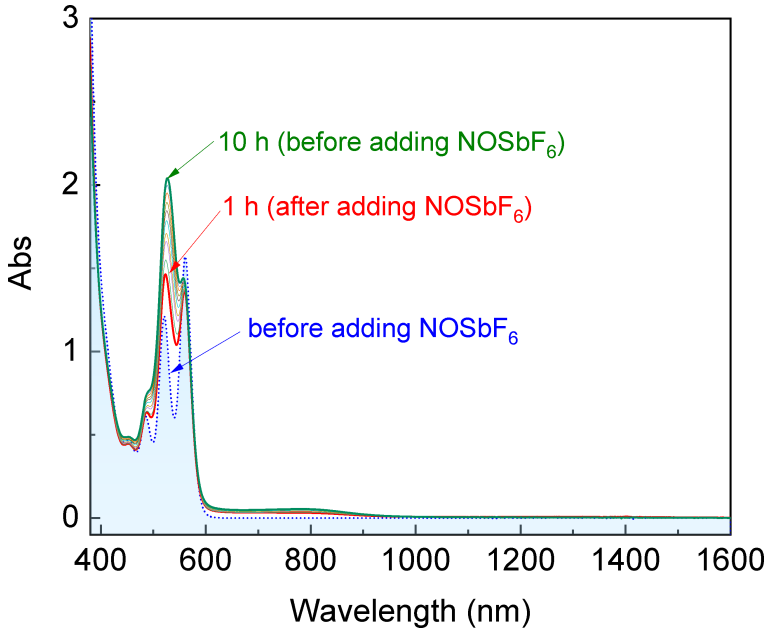

Figure S-45: UV-Vis-NIR spectra monitoring a solution of **6** (2.0×10^{-5} M) in undegassed, dry CH_2Cl_2 before and after addition of $NOSbF_6$ (4.5 mole equivalents). The solution was exposed to ambient light, maintained at room temperature, and monitored by UV-Vis-NIR analysis at 1-hour intervals.

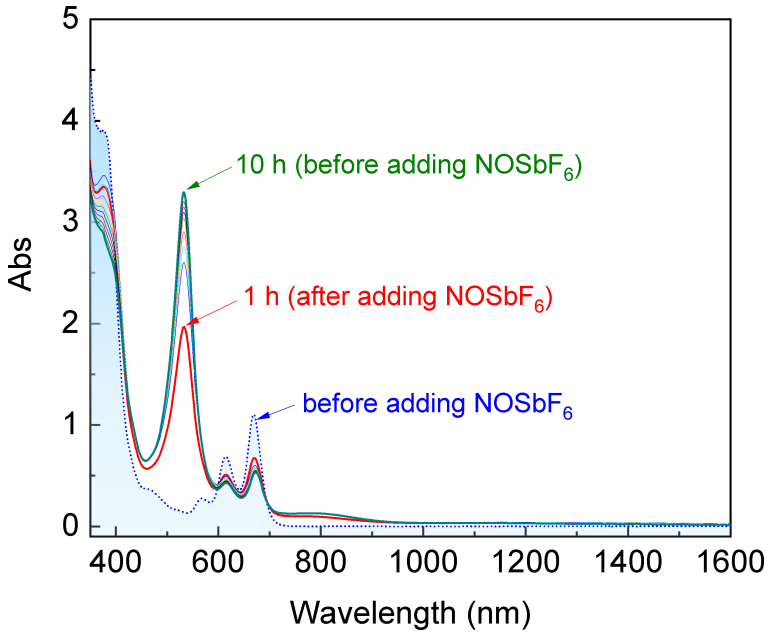

Figure S-46: UV-Vis-NIR spectra monitoring a solution of **9** (2.0×10^{-5} M) in undegassed, dry CH_2Cl_2 before and after addition of $NOSbF_6$ (4.5 mole equivalents). The solution was exposed to ambient light, maintained at room temperature, and monitored by UV-Vis-NIR analysis at 1-hour intervals.

8 Decomposition Kinetics of Large Acenes 12 and 14

8.1 Methodology

The first-order kinetic decays of the synthesized large acenes **12** and **14** can be evaluated by monitoring the changes in UV-Vis absorbance (A) of a given maximum absorption band as a function of time (t). Specifically, a decay process can be described by plotting $\log\left(\frac{A}{A_0}\right)$ against time (t), where A is the absorbance at time t and A_0 is the initial absorbance. The first-order decay equation is given by:

$$\log\left(\frac{A}{A_0}\right) = -k't$$

where $k' = \frac{k}{2.303}$ is the apparent rate constant in terms of base 10 logarithm, and k is the first-order rate constant. A linear fit of $2.303 \log\left(\frac{A}{A_0}\right)$ versus time t yields a slope of $-k$, from which the rate constant k can be obtained.

The half-life of a first-order reaction ($\tau_{1/2}$) can be determined directly from the rate constant k, using the following equation:

$$\tau_{1/2} = \frac{0.693}{k}$$

8.2 Results of Kinetic Analysis

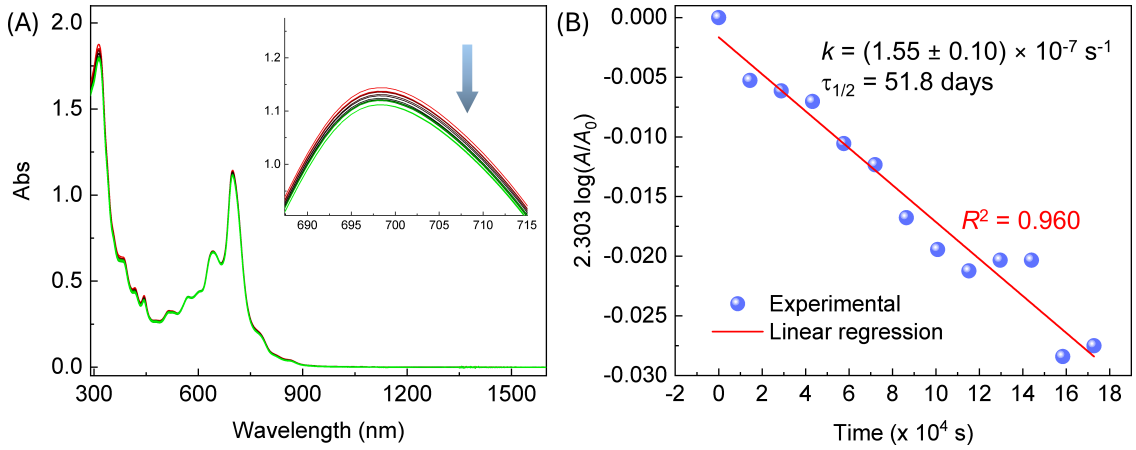

Figure S-47: (A) UV-Vis-NIR spectra monitoring a solution of **12** (5.0×10^{-5} M) in undegassed toluene exposed to ambient light at room temperature for 48 h. Inset: Expanded spectra around 699 nm. The arrow indicates a trend of decreasing intensity with time. (B) Kinetic plot of 2.303 log(A/A_0) against time (t), where A and A_0 are the absorbance measured at a time and the initial absorbance at 699 nm, respectively.

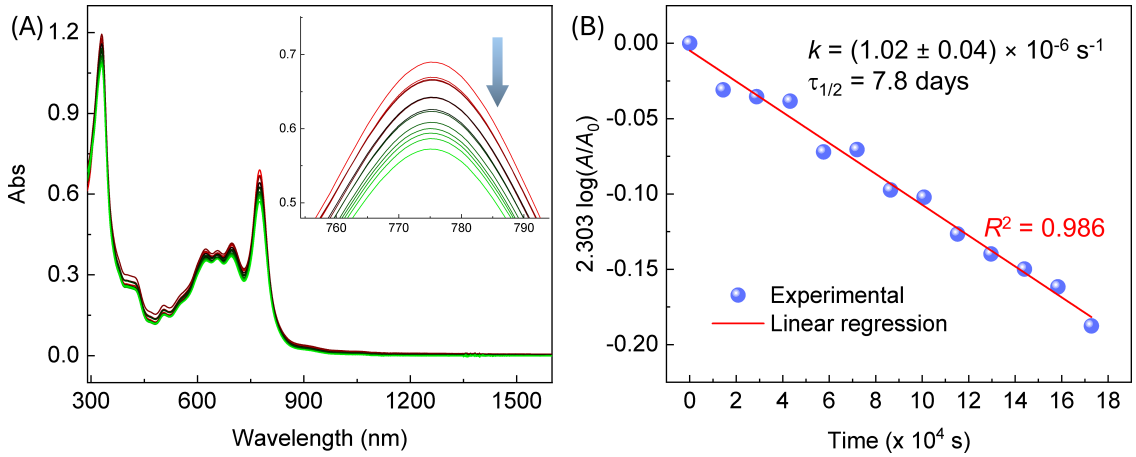

Figure S-48: (A) UV-Vis-NIR spectra monitoring a solution of **14** (3.0×10^{-5} M) in undegassed toluene exposed to ambient light at room temperature for 48 h. Inset: Expanded spectra around 775 nm. The arrow indicates a trend of decreasing intensity with time. (B) Kinetic plot of 2.303 log(A/A_0) against time (t), where A and A_0 are the absorbance measured at a time and the initial absorbance at 775 nm, respectively.

9 DFT Modeling Results for 14

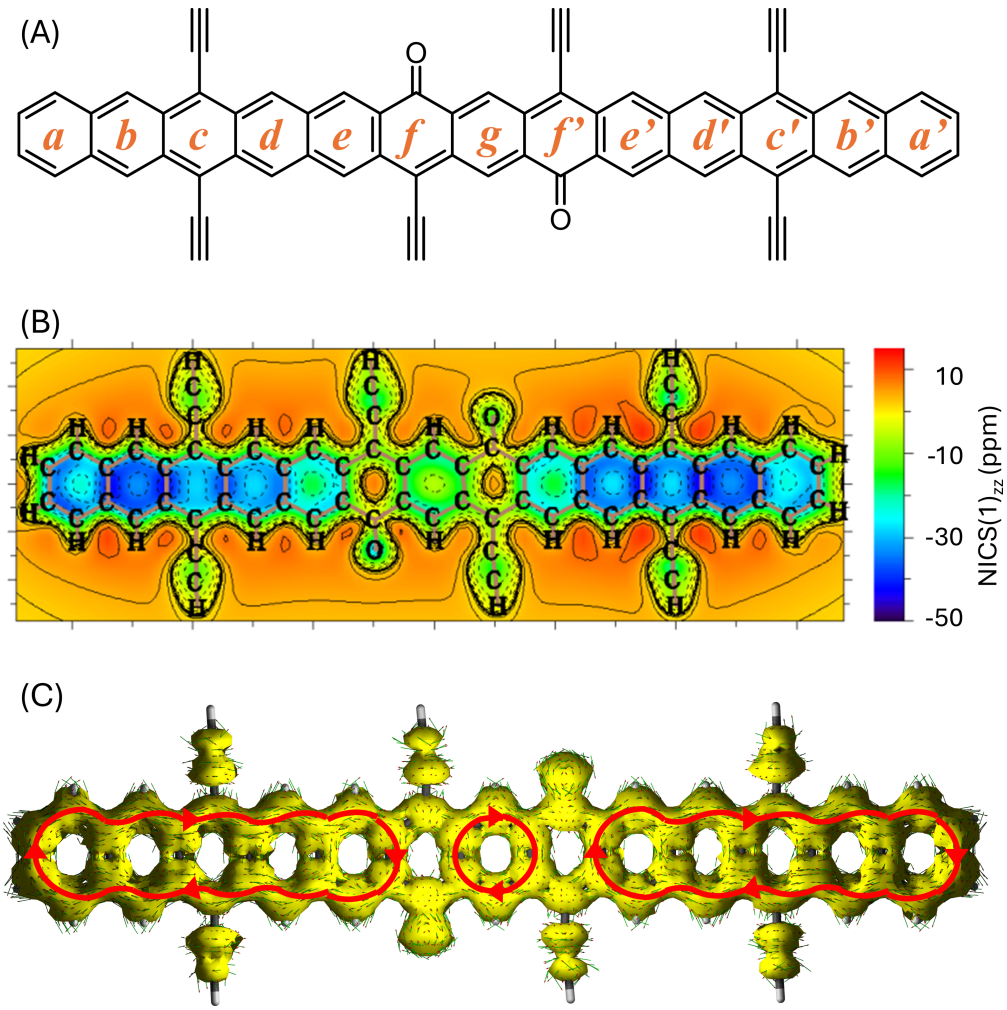

Figure S-49: (A) Molecular structure of a model tridecacene derived from **14** with each hexagonal ring is labeled. (B) Map of $NICS_{ZZ}$ above 1.0 Å of the tridecacene. (C) AICD plot of the tridecacene model. Calculations were done at the B3LYP/6-311+G(2d,p)level of theory in the singlet ground (S_0) state.

Table S-8: HOMA indexes for the hexagonal rings in **14**

Ring	**HOMA**	**Ring**	**HOMA**
a	0.637759	*e*	0.591558
b	0.736137	*f*	-0.085887
c	0.558438	*g*	0.714405
d	0.662279	–	–

10 Results of SQUID Analysis

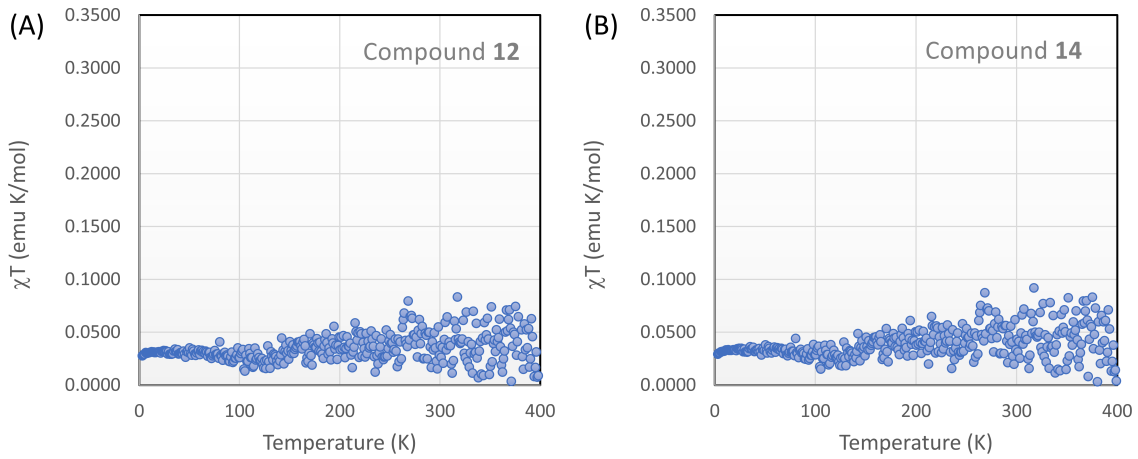

Figure S-50: Plots of χT versus T for compounds (A) **12** and (B) **14** determined from SQUID analysis in the solid state.

References

[1] Sheldrick, G. M. SHELXT–Integrated Space-Group and Crystal–Structure Determination. *Acta Crystallogr. A* **2015**, *71*, 3–8.

[2] Sheldrick, G. M. Crystal Structure Refinement with SHELXL. *Cryst. Struct. Commun.* **2015**, *71*, 3–8.

[3] Dolomanov, O. V.; Bourhis, L. J.; Gildea, R. J.; Howard, J. A.; Puschmann, H. OLEX2: A Complete Structure Solution, Refinement and Analysis Program. *Appl. Crystallogr.* **2009**, *42*, 339–341.

[4] Frisch, M. J. et al. Gaussian˜16 Revision C.01. 2016; Gaussian Inc. Wallingford CT.

[5] Wolinski, K.; Hinton, J. F.; Pulay, P. Efficient Implementation of the Gauge-independent Atomic Orbital Method for NMR Chemical Shift Calculations. *J. Am. Chem. Soc.* **1990**, *112*, 8251–8260.

[6] Cheeseman, J. R.; Trucks, G. W.; Keith, T. A.; Frisch, M. J. A Comparison of Models for Calculating Nuclear Magnetic Resonance Shielding Tensors. *J. Chem. Phys.* **1996**, *104*, 5497–5509.

[7] Lu, T.; Chen, F. Multiwfn: A Multifunctional Wavefunction Analyzer. *J. Comput. Chem.* **2012**, *33*, 580–592.

[8] Krygowski, T. M. Crystallographic Studies of Inter- and Intramolecular Interactions Reflected in Aromatic Character of π-Electron Systems. *J. Chem. Infor. Comput. Sci.* **1993**, *33*, 70–78.

[9] Ostrowski, S.; Dobrowolski, J. C. What Does the HOMA Index Really Measure? *RSC Adv.* **2014**, *4*, 44158–44161.

[10] Dobrowolski, J. C.; Ostrowski, S. On the HOMA Index of Some Acyclic and Conducting Systems. *RSC Adv.* **2015**, *5*, 9467–9471.